Science of the Total Environment 951 (2024) 175737

Contents lists available at ScienceDirect

Science of the Total Environment

journal homepage: www.elsevier.com/locate/scitotenv

Deep desert aquifers as an archive for Mid- to Late Pleistocene hydroclimate: An example from the southeastern Mediterranean

Roi Ram [a,b,c,*], Eilon M. Adar [a], Yoseph Yechieli [a,b], Reika Yokochi [d,†], Werner Aeschbach [c], Moshe Armon [e], D. Kip Solomon [f], Roland Purtschert [g], Alan M. Seltzer [h], Kerstin L. Urbach [c], Michael Bishof [i], Peter Mueller [i], Jake C. Zappala [i], Wei Jiang [j], Zheng-Tian Lu [j], Itay J. Reznik [b]

[a] Zuckerberg Institute for Water Research, Blaustein Institutes for Desert Research, Ben-Gurion University of the Negev, Sede-Boqer Campus, Israel
[b] Geological Survey of Israel, Jerusalem, Israel
[c] Institute of Environmental Physics, Heidelberg University, Heidelberg, Germany
[d] Department of the Geophysical Sciences, The University of Chicago, Chicago, IL, USA
[e] Institute for Atmospheric and Climate Science, ETH Zurich, Zurich, Switzerland
[f] Department of Geology and Geophysics, University of Utah, Salt Lake City, UT, USA
[g] Climate and Environmental Physics, Physics Institute, University of Bern, Bern, Switzerland
[h] Marine Chemistry & Geochemistry Department, Woods Hole Oceanographic Institution, MA, USA
[i] Physics Division, Argonne National Laboratory, Lemont, IL, USA
[j] Hefei National Laboratory, School of Physical Sciences, University of Science and Technology of China, Hefei, China

HIGHLIGHTS

- Unique long-term hydroclimate proxies are stored within deep desert aquifers.
- Varied hydroclimates are reflected in noble gas and water isotope compositions.
- Noble gas recharge temperatures reveal additional water sources along the flow path.
- Groundwater-based hydroclimate records support and enhance terrestrial archives.

GRAPHICAL ABSTRACT

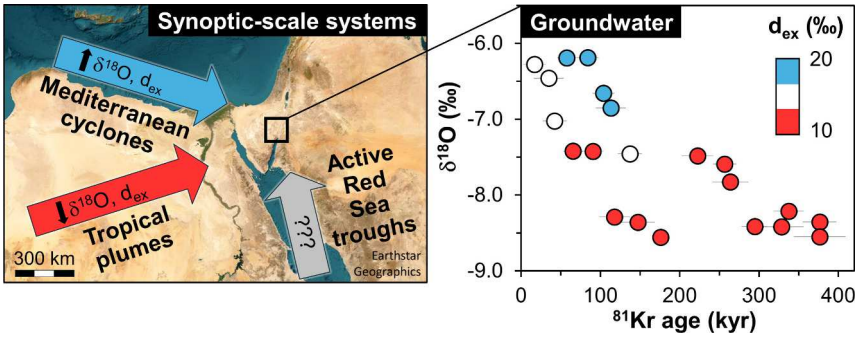

ARTICLE INFO

Editor: Jay Gan

Keywords:
Paleohydrology
Hydroclimate archives
Desert aquifers
Moisture sources

ABSTRACT

Many efforts have been made to illuminate the nature of past hydroclimates in semi-arid and arid regions, where current and future shifts in water availability have enormous consequences on human subsistence. Deep desert aquifers, where groundwater is stored for prolonged periods, might serve as a direct record of major paleo-recharge events. To date, groundwater-based paleoclimate reconstructions have mainly focused on a relatively narrow timescale (up to ~40 kyr), limited by the relatively short half-life of the widely used radiocarbon (5.73 kyr). Here we demonstrate the usage of deep regional aquifers in the arid southeastern Mediterranean as a hydroclimate archive for earlier Mid-to-Late Pleistocene epochs. State-of-the-art dating tools, primarily the ^{81}Kr

* Corresponding author at: Institute of Environmental Physics, Im Neuenheimer Feld 229, 69120 Heidelberg, Germany.
E-mail address: rram@iup.uni-heidelberg.de (R. Ram).
† Deceased in 2024.

https://doi.org/10.1016/j.scitotenv.2024.175737
Received 29 June 2024; Received in revised form 19 August 2024; Accepted 21 August 2024
Available online 24 August 2024

Recharge temperature
Excess air

radioisotope ($t_{1/2}$ = 229 kyr), were combined with other atmosphere-derived tracers to illuminate the impact of four distinguishable wetter episodes over the past 400 kyr, with differences in climatic conditions and paleo-recharge locations. Variations in stable water isotope composition suggest moisture transport from more proximal (Mediterranean) and distal (Atlantic) sources to different parts of the region at distinct times. Large variability in the computed noble gas-based recharge temperature (NGT), ranging ~15–30 °C, cannot be explained by climate variations solely, and points to different recharge pathways, including geothermal heating in the deep unsaturated zone and recharge from high-elevation (colder) regions. The obtained groundwater record complements and enhances the interpretation of other terrestrial archives in the arid region, including a contribution of valuable information regarding the moisture source origin as reflected in the deuterium-excess values, which is unattainable from the common practice analysis of calcitic cave deposits. We conclude that similar applications in other deep (hundred-m-order) regional groundwater systems (e.g., the Sahara desert aquifers) can significantly advance our understanding of long-term (up to 1 Myr) paleo-hydroclimate in arid regions, including places where no terrestrial remnants, such as cave, lake, and spring sediments, are available.

1. Introduction

Unveiling the history and sustainability of groundwater stored in deep aquifers across the world's desert belt, where the demand for water resources is rapidly increasing (e.g., Rödiger et al., 2023), is crucial for both present groundwater management and predictions of future trends. Many sub-tropical desert aquifers are dominated by old (pre-Holocene) groundwater, recharged during past pluvial episodes (Jasechko et al., 2017; Matsumoto et al., 2020; Purtschert et al., 2023; Sturchio et al., 2004). Valuable information regarding the prevailing hydroclimatic conditions during paleo-recharge can be obtained by coupling radioisotope-based tracer ages with other geochemical signals recorded in the groundwater. Among these are the dissolved noble gases, which are considered ideal natural tracers for paleo-hydrological studies owing to their chemical and biological inertness (e.g., Aeschbach-Hertig and Solomon, 2013; Stute and Schlosser, 2000; Weyhenmeyer et al., 2000).

Among other applications, measurements of dissolved Ne, Ar, Kr, and Xe concentrations have been widely used for the reconstruction of groundwater recharge temperatures (e.g., Aeschbach-Hertig et al., 2000; Bekaert et al., 2023; Seltzer et al., 2021). These tracers were also proven to be useful for the assessment of short and long-term water table fluctuation magnitude (Ingram et al., 2007; Ram et al., 2022). The latter can be reconstructed based on the amount of 'excess air' (commonly described in terms of excess neon) that results from air being trapped and dissolved when the water table rises (e.g., Aeschbach-Hertig et al., 2002; Aeschbach-Hertig and Solomon, 2013). Dissolved noble gases were largely combined in previous studies with the stable isotope composition of the water molecules, which ideally reflect synoptic-scale processes such as the rainstorm's moisture source and its track (e.g., Gat, 1996; Jouzel et al., 2013; Leguy et al., 1983; Priestley et al., 2020). The combination of these atmosphere-derived tracers enabled to underscore hydroclimatic shifts that have taken place around the Pleistocene-Holocene transition (e.g., Beyerle et al., 2003; Kulongoski et al., 2004; Weyhenmeyer et al., 2000). However, earlier hydroclimatic signals, which are potentially recorded in the groundwater archive, were not studied due to the lack of appropriate age tracers (in terms of timescale and complexity) beyond the ^{14}C dating range (e.g., Aeschbach-Hertig, 2014). Recent analytical advances in noble gas-based groundwater dating capabilities, and specifically, the development of and continual improvement in the Atom Trap Trace Analysis (ATTA) technique, now enable examination of groundwater recharge processes over a broad age spectrum, ranging from decades (^{85}Kr), through centuries (^{39}Ar), to the hundred-thousand-year timescale covered by the long-lived ($t_{1/2}$ = 229 kyr) ^{81}Kr radioisotope (Jiang et al., 2020; Ritterbusch et al., 2014; Zappala et al., 2020). This suite of age tracers, coupled with the stable noble gas and water isotope compositions, now provides an opportunity to examine hydroclimate signals preserved in old (100-kyr-timescale) groundwater.

The arid southeastern Mediterranean region is a place where expanding the paleo-hydroclimate toolbox is crucial. The region is characterized by a steep rainfall gradient southward and away from the Mediterranean Sea (e.g., Enzel et al., 2008), and extreme hyperaridity (< 50 mm/yr) currently prevails over most of the Negev and Sinai Peninsula deserts (Israel and Egypt, respectively; Fig. 1a). Aridosols (desert soils) from the southern Negev were used to propose a continuous long-term (~1 Myr) hyperaridity over the region (Amit et al., 2011, 2006), whereas cave deposits (speleothems) were used to suggest intermittent, short-term and extremely wet (> 300 mm/yr) episodes, which could have also provided a temporary migration corridor for humans and animals between Africa and the Levant (Vaks et al., 2010, 2007). Groundwater has the potential to complement and enhance the interpretation of such near-terrestrial records. For instance, hydroclimatic information generated by stalagmite and stalactite deposition provides high-resolution, time- and site-specific hydroclimatic insights in places where water was able to infiltrate into a pre-existing cave and surpass the speleothem deposition threshold (e.g., Fleitmann et al., 2007; Tadros et al., 2019; Vaks et al., 2010). In contrast, information from regional aquifers spatially average extended recharge areas, including surface water that could be driven to the recharge area from far-away floods. Furthermore, groundwater archives preserve the isotope composition of the infiltrating water and, therefore, enable the examination of the moisture source origin. On the other hand, groundwater age resolution is much lower compared to that of speleothems. Additionally, regional groundwater systems may suffer from mixing (e.g., Atencio et al., 2024), that can mask the signal of 'individual' recharge components. These complications need to be carefully taken into account while interpreting data obtained in such natural systems.

This study aims to examine further the hydroclimatic history of the arid southeastern Mediterranean and expand current groundwater-based paleoclimatology by applying atmosphere-derived geochemical tracers in multiple deep groundwater systems. The coupling of long-term radioisotope age tracers with stable noble gas and water isotope compositions enabled identification of the impact of multiple recharge episodes in the groundwater archive. Furthermore, the distinct isotope signatures recorded in the groundwater provided insights into the differential impact of synoptic-scale systems under varied hydroclimatic conditions. The integration of the obtained groundwater-based hydroclimate record with proximal and more distal terrestrial archives allowed further unraveling of the nature and spatial patterns of paleo-precipitation.

2. Study area

2.1. Hydrogeological background

Two deep regional groundwater systems – the Kurnub Gr. Nubian sandstone and the overlying Judea Gr. carbonate (Lower and Upper Cretaceous; hereafter referred to as the sandstone and carbonate aquifers, respectively) are found below the Sinai (Egypt) and Negev (Israel) deserts (Fig. 1a). The study of these transboundary aquifers has been ongoing for more than half a century (e.g., Arad and Kafri, 1980; Issar et al., 1972; JICA, 1999; Vengosh et al., 2007) and enabled the

development and groundwater production in dozens of wells. Fresh to slightly brackish groundwater is produced along the Arava Valley margins (Fig. 1a) and enables agriculture to thrive despite the harsh arid environment. Bounded by the Dead Sea Transform fault system, the Arava Valley extends between the Gulf of Aqaba (Eilat) in the south and the terminal Dead Sea in the north. The Notza ridge (Fig. 1b) constitutes the surface watershed between these two drainage bases and, in the frame of the present study, defines the northern boundary (ca. 30° 09′ N) of the Southern Arava Valley (SAV) sub-basin. Extreme hyperaridity prevails over the SAV, with an average precipitation of <40 mm/yr and hot summers (daily max temperatures frequently reach 40 °C) (Goldreich, 2003; Goldreich and Karni, 2001).

Previous works outlined the sandstone aquifer's flow structure (Guttman et al., 1999; Issar et al., 1972; JICA, 1999; Kroitoru, 1980) from the southern recharge area in Sinai, where the sandstone vastly outcrops (Fig. 1a), through the bottleneck dictated by the Themed Fault at the Nekhel area, to the natural outlets found to the west (the Gulf of Suez) and east (the Gulf of Aqaba and the Dead Sea) (Fig. 1a). The groundwater flow splits in two in the southern Negev (arrows in Fig. 1b). One flow component is diverted northeast toward the Dead Sea, and the second flows east and enters the Southern Arava Valley (SAV) while crossing a series of faults (Fig. 2a) and downfaulted blocks (Guttman et al., 1999; Issar et al., 1972). A similar flow pattern is assumed for the overlying carbonate aquifer, for which a thick sequence of shales (Ora Fm.; Fig. 2b) divides the group into lower and upper sub-aquifers (Guttman et al., 1999). Shales also appear at the bottom of the Judea Gr. and hydrologically separate the two regional aquifers, even though evidence for partial connectivity was proposed in places (Arad and Kafri, 1980; Atencio et al., 2024; Rosenthal et al., 2007). The Judea Gr. rocks are more vastly exposed throughout the basin (Fig. 1a), and therefore, some additional recharge areas are found along the aquifer's flow paths.

Within the SAV, the regional aquifers discharge into a local aquifer composed of clastic sediments of various grain sizes, which were deposited in the rift valley since the Neogene era (hereafter defined as the alluvial aquifer). The alluvial aquifer is also fed from the east (dashed arrows in Fig. 1b and c) by infiltration of floodwater at the foothills of the 1.5-km-high Edom Mountains (southwestern Jordan), where a somewhat wetter and milder climate prevails (Adar et al., 1992; Bein et al., 2001; Rosenthal et al., 1990). Groundwater flow in the SAV is generally directed south toward the Gulf of Aqaba outlet (Guttman et al., 1999; Naor et al., 2004).

2.2. Hydroclimatic background

Groundwater recharge in many desert aquifers is governed by deep percolation following short-term flash floods (e.g., Purtschert et al., 2023; Scanlon et al., 2006; Shentsis and Rosenthal, 2003; Sultan et al., 2011). Modern-day floods in the Sinai and Negev deserts are generated by different synoptic-scale systems that transport moisture from various origins, including Mediterranean Cyclones (MCs), which largely transport moisture from the Mediterranean Sea, tropical plumes, which carry moisture from the tropical Atlantic, and active Red Sea troughs, which transport moisture from other southern sources, including the Red and Arabian seas (Armon et al., 2019, 2018; de Vries et al., 2013; Kahana et al., 2002; Rubin et al., 2007). Low recharge rates (~1–10 mm/yr order), associated with the current hyperarid climate, were estimated for the regional aquifers (Guttman et al., 1999; Issar et al., 1972; Kroitoru, 1980; Sultan et al., 2011). This was further corroborated by prolonged groundwater residence times, on the order of tens to hundreds of thousands of years (e.g., Ram et al., 2021; Yokochi et al., 2019). The low current recharge rates and the elevated residence times indicate that the main recharge has taken place during past, more pluvial periods,

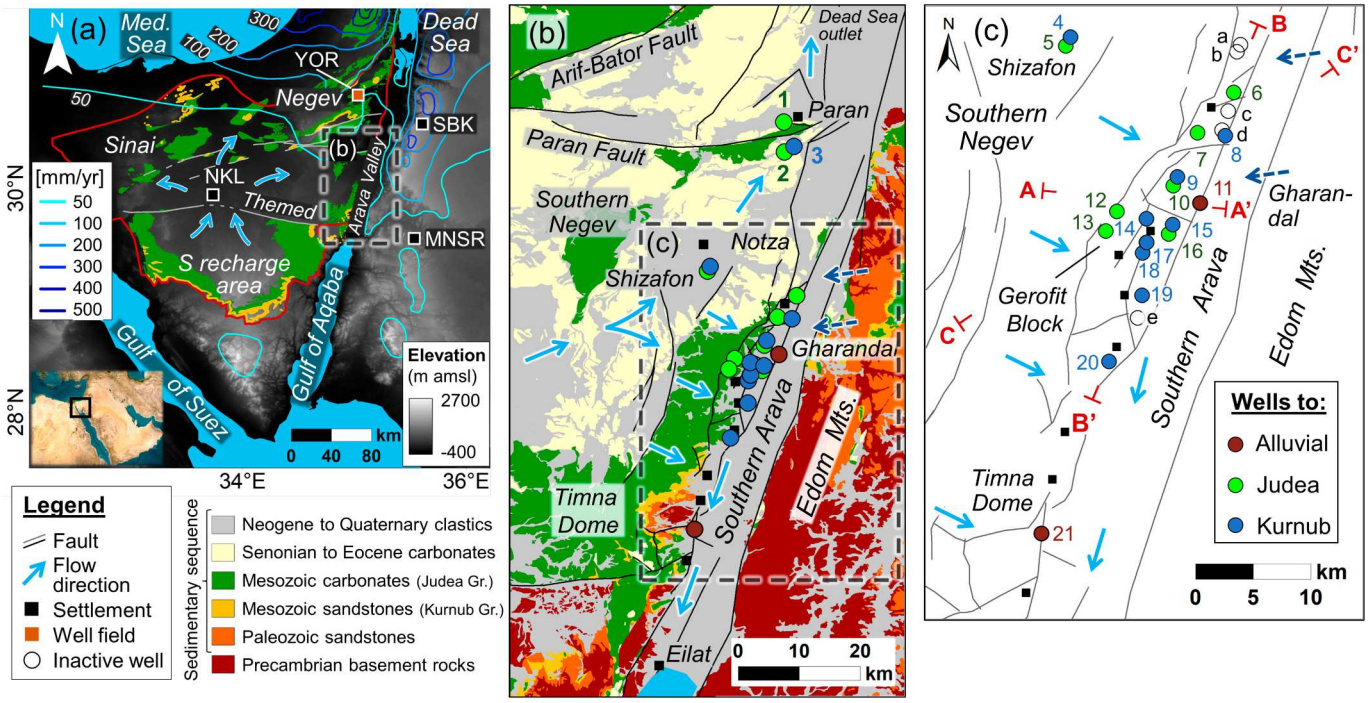

Fig. 1. (a) Main flow directions (arrows) and outcrops (colored polygons) of the two deep regional groundwater systems of the Sinai-Negev Basin, including the sandstone (Kurnub Gr.) and the carbonate (Judea Gr.) aquifers. Grey lines are major faults, and a red line denotes the approximate boundaries of the sandstone aquifer (adopted from Ram et al., 2020). Isohyets are modified after Armon et al. (2018); Enzel et al. (2008); and Kushnir et al. (2017). The 50 mm/yr isohyets were interpreted using the WorldClim v2.1 dataset (Fick and Hijmans, 2017). NKL - Nekhel; MNSR – Manshir; SBK – Shoubak; YOR - Yorkeam. (b) Location of wells and schematic flow directions, shown on a generalized geological map of the Southern Arava Valley (SAV) and its surroundings (Eyal et al., 1980; Sneh et al., 1998). Dashed arrows indicate contribution to groundwater in the SAV from the slopes of the Edom Mountains. (c) Enlarged map of the SAV, with wells, faults (lines), and cross-section locations (C-C′ appears in Sup. Fig. B.1). Well IDs (Table 1) are color-coded according to the aquifer. Also shown are inactive wells that appear in Fig. 2b, including Notza 1, Notza 11, Yaalon 5, Yaalon 6, and Gerofit 5 (a-e, respectively).

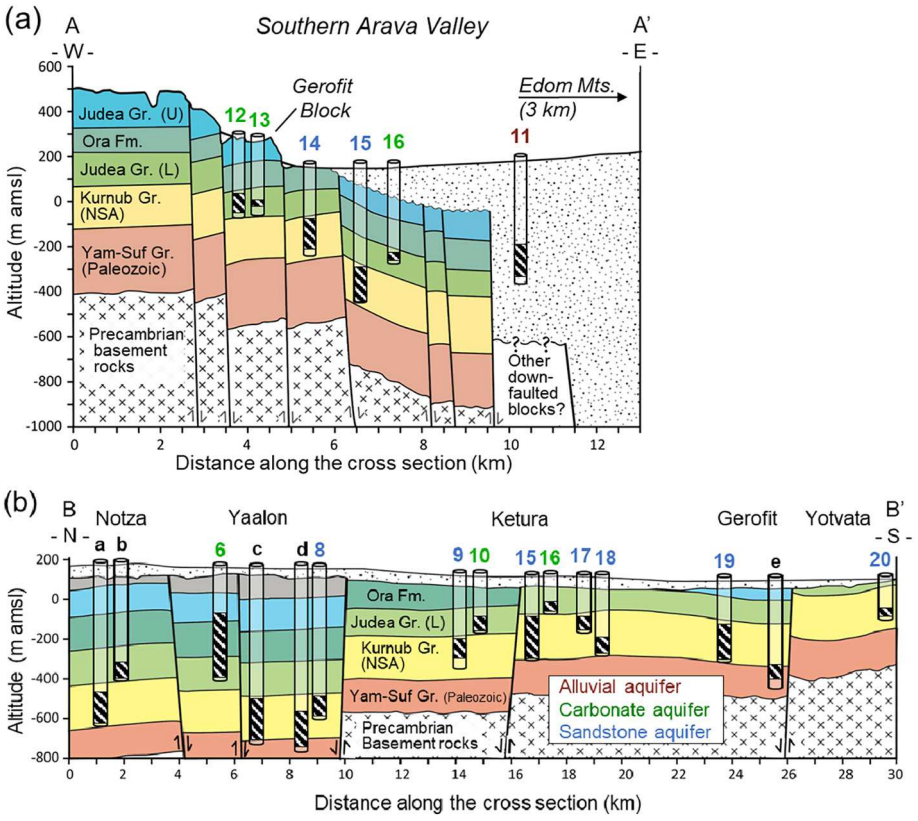

Fig. 2. Schematic cross sections, (a) perpendicular to and (b) along the Southern Arava Valley, with screen intervals (black stripes) for each well. Cross-section and well locations, including inactive wells (a-e), are presented in Fig. 1c. Well IDs (Table 1) are color-coded according to the aquifer (see legend). Cross-sections are modified after Burg et al. (2013); Kroitoru et al. (1981); Naor et al. (2004); and Fleischer and Gafsou (2003).

probably as a result of an increase in the frequency and/or the magnitude of extreme weather events and consequent floods (e.g., Armon et al., 2018; Kahana et al., 2002).

The timing, climate, and spatial distribution of past wet periods over the study area have been examined through various records. A long-term hyperaridity (< 80 mm/yr) was proposed for the southern Negev over the past million years based on well-developed gypsic-salic reg soils (Amit et al., 2011, 2006). However, cave deposits from this region suggest short-term wetter episodes during the mid-to-late Pleistocene interglacials (Vaks et al., 2010, 2007), with the Mediterranean Sea as the proposed main source of precipitation (Vaks et al., 2018, 2010). Similarly, wetter interglacial episodes were deduced from other speleothem records in the northeastern part of the Sahara (Egypt), ca. 400 km southwest of the Negev Desert caves (El-Shenawy et al., 2018; Henselowsky et al., 2021). These wetter interglacial episodes were suggested to be related to a northward shifting of the West African Monsoons (El-Shenawy et al., 2018) as well as possible larger precipitation from MCs, tropical plumes, and active Red Sea troughs (Henselowsky et al., 2021). Information gathered from stable water isotopes in rainwater and groundwater over the northeastern Sahara suggested however that wetter periods occurred during glacial, rather than interglacial, epochs, with the Atlantic as the proposed main moisture source (Abouelmagd et al., 2012; Sonntag et al., 1980; Sultan et al., 1997).

Recent applications of the ^{81}Kr and ^{14}C age tracers in the sandstone aquifer support increased precipitation and groundwater recharge over the northern Negev during the Last Glacial Period (LGP), with a proposed major recharge during the late (< 40 kyr) LGP (Ram et al., 2020; Yokochi et al., 2019). Relatively high δ^2H and δ^{18}O values (ca. -6.5 and -30 ‰, respectively), as well as high deuterium-excess ($d_{ex} = \delta^2$H-8 × δ^{18}O) values of ca. 20 %, characterize the northern Negev LGP groundwater. These values were proposed as indicators for dominant paleorecharge by MCs (Yokochi et al., 2019). An earlier, Mid-Pleistocene wet episode seems to dominate the southern Negev groundwater and was related to paleo-recharge over the southern recharge area in Sinai (Fig. 1a) ca. 360 ± 30 kyr ago (Ram et al., 2020; Yokochi et al., 2019). Dominant transportation of moisture by tropical plumes during a colder and wetter climate was proposed for the latter episode based on low δ^2H, δ^{18}O, and d_{ex} values (ca. -8.5, -55, and 10 ‰, respectively; Yokochi et al., 2019). Notably, the considerable age uncertainty (± 30 kyr) for the timing of this reconstructed wet episode includes both glacial and interglacial epochs (Marine Isotope Stages 11 to 9). The 300–400 kyr old groundwater also carries unique dissolved noble gas signals, including high noble gas concentrations that highlight large entrapment and dissolution of air bubbles as a result of a long-term water-table rise during this pluvial episode (Ram et al., 2022). A rigorous examination of noble gas and water stable isotope compositions of groundwater from multiple deep aquifers in the southern Negev and the SAV was conducted in the current study to investigate additional groundwater recharge episodes and broaden our hydroclimatic understanding of patterns and origins of paleo-precipitation in the arid region.

3. Materials and methods

Groundwater samples were collected for various geochemical analyses in deep (> 100 m below surface) boreholes over the southern Negev and the SAV, including twenty production wells and a single observation well (Sup. Table A.1). The sampled wells are characterized by long (tens to hundreds of m) screen intervals (Sup. Table A.1). Dissolved gases were extracted in-situ from the pumped groundwater using a field-degassing apparatus (Yokochi, 2016). Kr was separated from the extracted gas and then measured for both ^{81}Kr and the shorter-lived ^{85}Kr ($t_{1/2}$ = 10.7 yr) radioisotopes relative abundance using an ATTA-3

instrument (Jiang et al., 2012; Zappala et al., 2020) at the Tracer Center (Argonne National Laboratory, USA) and Hefei National Laboratory (China). The measured ^{81}Kr activity, presented in percent of modern atmospheric Kr (pmKr), was converted into ^{81}Kr tracer age using the radioactive decay law (e.g., Purtschert et al., 2023). ^{14}C measurements were conducted in two sample types: Water samples, collected for standard dissolved inorganic carbon (DIC) analysis, and extracted gas samples, from which CO_2 was later separated (Yokochi et al., 2018). Radiocarbon analyses were performed using accelerator mass spectrometry facilities at the University of Georgia (USA), GNS Science (New Zealand), and the University of Arizona (USA) laboratories. Additional samples were collected and analyzed for water stable isotope composition at the Zuckerberg Institute for Water Research (ZIWR, Israel) using the cavity ring-down spectroscopy technique, with a reported standard deviation of 0.1 and 0.5 ‰ (versus Vienna Standard Mean Ocean Water; VSMOW) for δ^{18}O and δ^{2}H, respectively. Chloride content was measured at the Geological Survey of Israel and the ZIWR labs, with a measurement error of 2 %.

Samples for dissolved noble gas contents (Ne, Ar, Kr, Xe) were collected in standard copper tubes (e.g., Aeschbach-Hertig and Solomon, 2013) and measured at the University of Utah (USA) and Heidelberg University (Germany). Noble gas recharge temperature (NGT) and excess Ne (ΔNe) amount (i.e., the percent supersaturation of dissolved neon) were computed using the PANGA software (Jung and Aeschbach, 2018) under the assumption of a closed-system equilibration (CE) between water and atmospheric air (Aeschbach-Hertig et al., 2000). Input parameters for the CE modeling were adopted from Ram et al. (2022), including salinity of 1 ‰ and recharge elevation (i.e., water table elevation) of 300 m above sea level, which is based on current water tables upstream of the regional aquifers in Sinai (JICA, 1999). Despite the uncertainty in the estimation of paleo recharge elevation (e.g., water levels could have been higher during wetter episodes, and, in contrast, lower recharge elevations can be anticipated for the carbonate aquifer's potential recharge areas located downstream in the southern Negev), we note that ±200 m change in the recharge elevation (air pressure) will only minorly affect the CE modeling results, with a difference of less than 1 °C in the computed NGTs (Sup. Fig. A.1). 1000 Monte Carlo fits per sample were carried out with the PANGA software using the Ne, Ar, Kr, and Xe contents (Sup. Table A.2), with resulting fair fitting (low X^2) of the model parameters for most of the samples (sup. Table A.3). A few samples for which relatively large NGT uncertainty (> 4 °C) was obtained were further assessed by restricting the Monte Carlo simulation results to realistic clusters solely (i.e., physically plausible parameter values; Jung et al., 2013; Jung and Aeschbach, 2018).

4. Results

A wide range of ^{81}Kr activities, between 30 and 85 pmKr, was obtained for the sandstone aquifer over the southern Negev and the SAV, whereas a narrower range of 60–95 pmKr was measured in the overlying carbonate aquifer (Table 1). These ranges are correlative to ^{81}Kr tracer ages of a few tens to a few hundreds of thousands of years (Fig. 3). Lower ^{81}Kr activities, correlative to older groundwater ages, were obtained in the sandstone aquifer compared to that in the overlying carbonate aquifer wherever adjacent wells (a few tens of m apart) were available for the sampling (e.g., wells 2 and 3; Table 1). Low ^{14}C activities, mostly below 1 % of modern carbon (pMC; Table 1), were detected in the various aquifers, providing additional evidence for the prolonged (10^4-yr-timescale or longer) groundwater residence time. Low activity was also obtained for the shorter-lived ^{85}Kr radioisotope, with measured values mostly below one dpm/cc (Table 1). These values constitute <1 % of the current atmospheric ^{85}Kr activity over the study area (Ram

Table 1
Chloride, water stable Isotopes, radioisotope compositions, ^{81}Kr ages, and noble gas dissolution modeling results in the southern Negev and Arava Valley groundwater. For well locations, see Fig. 1c.

#	Well Name	Aquifer	Cl^-	H_2O isotopes		d_{ex}	radioisotope data and computed ^{81}Kr ages				CE modeling results [a]	
				δ^{18}O	δ^{2}H		^{81}Kr	Age	^{85}Kr	^{14}C[b]	DNe	NGT
			mg/L	‰ VSMOW			pmKr	kyr	dpm/cc	pMC	‰	°C
Southern Negev												
1	Paran 21[c]	Carbonate	487	−7.42	−46.1	13.3	76 ± 3	91 ± 13	0.38 ± 0.15	*< 0.2*	28 ± 3	27.2 ± 1.2
2	Paran 129[c]	Carbonate	551	−7.42	−47.4	12.0	82 ± 3	66 ± 12	< 0.42		21 ± 3	24.8 ± 1.0
3	Paran 29[c]	Sandstone	742	−8.36	−56.1	10.7	32 ± 2	376 ± 21	< 0.45	0.5 ± 0.3		
4	Shizafon 1[c]	Sandstone	599	−8.41	−56.8	10.5	41 ± 2	295 ± 17	< 0.49	0.7 ± 0.3	501 ± 15	24.2 ± 2.1
5	Shizafon 11[c]	Carbonate	610	−7.48	−47.5	12.4	51 ± 3	222 ± 20	< 0.85	*< 0.2*	49 ± 3	29.7 ± 1.7
Southern Arava Valley												
6	Yaalon 117	Carbonate	398	−7.02	−40.4	15.8	88 ± 4	42 ± 15	< 0.52	*< 0.2*	50 ± 3	23.4 ± 1.6
7	Yaalon 1a	Carbonate	452	−7.46	−44.8	14.9	66 ± 3	137 ± 15	0.42 ± 0.08	*< 0.3*		
8	Yaalon 6b	Sandstone	272	−6.19	−29.6	20.0	84 ± 3	58 ± 12	< 0.65	*1.5 ± 0.1*	27 ± 3	14.4 ± 1.1
9	Ketura 9[c]	Sandstone	320	−6.85	−36.5	18.3	71 ± 4	113 ± 19	< 0.83	*0.6 ± 0.1*	62 ± 4	18.5 ± 1.1
10	Ketura 19	Carbonate	354	−6.28	−35.7	14.5	95 ± 4	17 ± 14	0.69 ± 0.18	*0.5 ± 0.1*	7 ± 1	26.6 ± 0.6
11	Yaalon 8	Alluvial	606	−6.19	−30.3	19.2	79 ± 3	84 ± 14[d]	5.28 ± 0.30	2.9 ± 0.1	25 ± 1	15.3 ± 0.4
12	Ketura 6	Carbonate	545	−8.36	−55.2	11.7	64 ± 4	147 ± 21	< 0.66	*< 0.2*	164 ± 6	31.2 ± 2.0
13	Ketura 7	Carbonate	532	−8.56	−56.3	12.1	59 ± 2	176 ± 11	0.88 ± 0.21	< 0.3		
14	Yaalon 3a[c]	Sandstone	622	−8.42	−56.7	10.6	37 ± 3	328 ± 28	< 0.51	*< 0.2*		
15	Ketura 5	Sandstone	580	−6.66	−36.5	16.7	73 ± 3	104 ± 14	< 0.28		61 ± 1	16.9 ± 0.4
16	ketura 115[c]	Carbonate	475	−6.46	−37.6	14.1	90 ± 5	35 ± 19	< 0.27	*0.5 ± 0.1*	27 ± 1	24.9 ± 0.6
17	Ketura 14	Sandstone	483	−7.83	−49.5	13.1	45 ± 3	264 ± 23	< 0.38		190 ± 2	19.6 ± 0.6
18	Ketura 4a[c]	Sandstone	733	−8.21	−54.4	11.3	36 ± 2	338 ± 19	< 0.50	0.4 ± 0.1	310 ± 10	27.7 ± 2.1
19	Gerofit 4[c]	Sandstone	981	−7.59	−47.7	13.1	46 ± 2	257 ± 15	< 0.44	0.6 ± 0.1[e]	339 ± 11	27.4 ± 2.4
20	Yotvata t/9[c]	Sandstone	743	−8.55	−56.9	11.5	32 ± 3	376 ± 33	0.38 ± 0.09		329 ± 11	29.8 ± 2.2
21	Timna 6b	Alluvial	2420	−8.29	−56.2	10.1	70 ± 4	118 ± 19	0.95 ± 0.43	*0.9 ± 0.1*	37 ± 3	30.3 ± 1.7

[a] Noble gas contents are provided in Sup. Table A.2 and the extended model output is summarized in Sup. Table A.3.
[b] ^{14}C measured in CO_2 gas samples are in *italics*. Others were measured in water samples (see Methods). The laboratory where each measurement was performed is detailed in Sup. Table A.4.
[c] Isotope compositions and ^{81}Kr ages are from Yokochi et al. (2018, 2019) and Ram et al. (2020, 2021).
[d] ^{81}Kr age corrected for atmospheric contamination as described in Purtschert et al., 2021 (See Sup. Note B.1).
[e] From Vengosh et al. (2007).

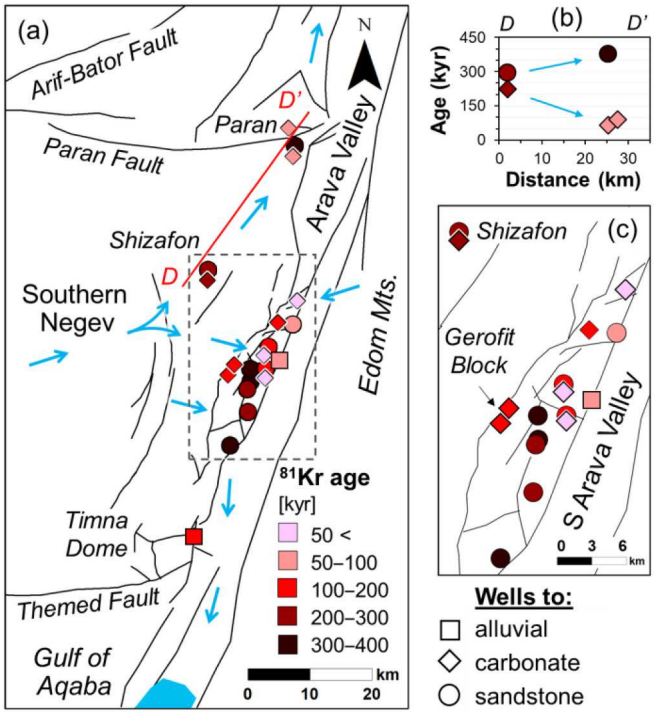

Fig. 3. ^{81}Kr ages in the southern Negev and Arava Valley aquifers. Arrows indicate the main groundwater flow directions and solid lines mark faults. Subfigure b shows the opposite ^{81}Kr age trends in the two regional aquifers along the flow path from Shizafon toward Paran (D-D′). Note the scale of the maps and the high age heterogeneity in the Southern Arava Valley surroundings (subfigure c).

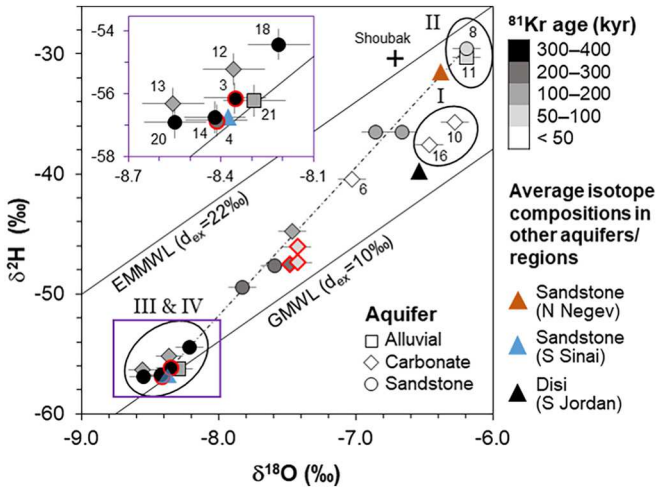

Fig. 4. Water stable isotope compositions in the studied aquifers. Solid lines are the global and local (East Mediterranean) meteoric water lines, with deuterium-excess (d_{ex}) values of 10 and 22 ‰, respectively (Gat and Dansgaard, 1972). Groundwater samples collected in the southern Negev (i.e., away from the SAV), including the Shizafon and Paran wells (Fig. 1b), are marked with a red outline. Triangles mark average isotopic compositions observed in other parts of the sandstone aquifer (location shown in Fig. 1a), including the Nekhel area in south-central Sinai (Abouelmagd et al., 2014; JICA, 1999) and Yorkeam wells in the northeastern Negev (Ram et al., 2020). Also shown are average isotopic compositions in Jordan (for location, see Fig. 1a), including in the Disi Aquifer in the Manshir area (black triangle; El-Naser and Gedeon, 1996) and that of rainwater over the Edom Mountains in Shoubak weather station (black cross; Bajjali, 2012). The dashed line demonstrates a mixing pattern in the sandstone aquifer among the proposed two dominant components. The impact of multiple pluvial periods, which have occurred at different times and under varying climates, is reflected in the marked four clusters (ellipses) with dissimilar ^{81}Kr-δ^{18}O-δ^{2}H combinations (groups I–IV). δ^{2}H measurement errors are smaller than the symbol size.

et al., 2021), in accordance with the ancient nature of the groundwater. An exception is well #11, where a higher ^{85}Kr activity was obtained (6 % of the current atmospheric value) and seems to result from air contamination (see Supplementary Note B.1 for further information). This well also presents a slightly elevated ^{14}C activity (3 pMC; Table 1), as measured in two different samples collected five years apart (Supplementary Note B.1). Together with the ^{81}Kr information, the slightly elevated ^{14}C activity demonstrates a mixture of older and somewhat younger groundwater components in the alluvial aquifer.

The studied aquifers also have a range of water stable isotope compositions, with δ^{18}O and δ^{2}H values ranging between -8.5 to -6.0 ‰ and -60 to -30 ‰, respectively (Table 1). Noticeably, samples with a more depleted (negative) isotopic composition are characterized by low d_{ex} values of 10–12 ‰, resembling that of average global meteoric waters (Fig. 4), whereas samples with the highest δ^{18}O and δ^{2}H values fall closer to the East Mediterranean meteoric water line (d_{ex} of 22 ‰; Gat and Dansgaard, 1972). Large variability is also reflected in the concentration of the dissolved noble gases (Sup. Table A.2). For instance, Ne content ranges mostly between 2.1 and 7.5 × 10^{-7} ccSTP/g, which corresponds to an enrichment of up to a few hundred percent relative to air-saturated water (ΔNe values; Table 1).

Fresh to brackish groundwater is encountered in the studied aquifers, with Cl^- content mainly ranging between 250 and 1000 mg/L (Table 1). A relatively low Cl^- content of ca. 300 mg/L was obtained in the northern part of the SAV, where the youngest groundwater is encountered, whereas southward, salinity generally increases (Fig. 5a). An order of magnitude higher salinity (~2500 mg Cl^- L^{-1}) was obtained in the southernmost among the sampled wells (#21), which taps the alluvial aquifer east of the Timna Dome (Fig. 1c). Highly brackish and even saline groundwater was also encountered locally in other parts of the SAV (Bein et al., 2001; Kroitoru et al., 1981; Naor et al., 2004; Vengosh et al., 2007), but mainly in wells that intruded the deeper Paleozoic aquifer (e.g., wells d and, e; Fig. 2b). In the Timna Dome area, the combination of increased salinity and low δ^{18}O value, as observed in Well #21 (Fig. 5a and b), was hypothesized to reflect flushing of brine remnants by meteoric waters originating from the regional aquifers (Bein et al., 2001). A small contribution of a brine component (in the order of a few percent) can potentially dominate the ionic composition (e.g., Cl^- content), whereas its impact on the water isotope composition, as well as the noble gas bulk contents and radioisotope activities, is expected to be minor (e.g., Gerber et al., 2017; Ram et al., 2020).

5. Discussion

5.1. Age and isotope composition spatial variations

Old groundwater (mostly >50 kyr) dominates the southern Negev and the SAV, as demonstrated by the ^{81}Kr age distribution over the study area (Fig. 3a). The scatter in ^{81}Kr ages and water stable isotope compositions (Fig. 4) indicates that the studied aquifers store waters of different origins, both in terms of time and climatic conditions during the paleo-recharge. Together, measurements of sub-modern ^{81}Kr activities along with near-zero ^{14}C activities and an absence of ^{85}Kr (Table 1), provide evidence for the lack of a significant contribution of Holocene-age recharge over the study area. The pronounced ^{81}Kr age decrease of ca. 150 kyr in the carbonate aquifer between the Shizafon and Paran wells (Fig. 3b) indicates significant recharge from relatively young (< 100 kyr) groundwater dating back to the Late Pleistocene. This stands in contrast to the identified aging of ca. 80 kyr in the underlying sandstone aquifer over the same flow segment (Fig. 3b). These opposite trends highlight that the carbonate aquifer receives some additional contribution of younger recharge, while the deeper sandstone aquifer seems to

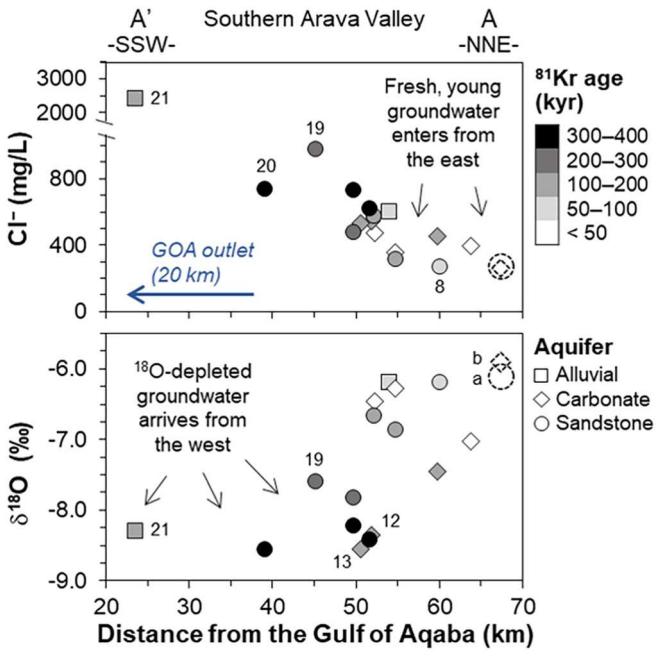

Fig. 5. Spatial variations in (a) Cl^- content and (b) $\delta^{18}O$ values of groundwater along the Southern Arava Valley. Wells (Table 1) are presented as a function of distance from the Gulf of Aqaba/Eilat (GOA) terminal outlet. Measurement errors for both $\delta^{18}O$ and Cl^- are smaller than the symbol size. $\delta^{18}O$ and Cl^- data for the two Notza wells (a and b wells in Fig. 1c) were taken from Naor et al. (2004).

remain isolated (confined) along this flow path.

Notably, the sandstone aquifer's 300–400 kyr old groundwaters in the southern Negev and the SAV are characterized by low $\delta^{18}O$ and δ^2H values (Group IV in Fig. 4). A similar isotopic composition, which falls close to the Global Meteoric Water Line (GMWL; Fig. 4), was detected in ^{14}C-depleted groundwater found upstream of the sandstone aquifer in south-central Sinai (Fig. 4; Abouelmagd et al., 2014; Issar et al., 1972; JICA, 1999). The homogeneity in the isotopic composition along a flow segment of ca. 150 km, stretching from the Nekhel area (Fig. 1a) to the Arava Valley margins, supports a common origin for the groundwater in terms of the prevailing hydroclimatic conditions during the paleo recharge, which were likely very different from present-day conditions; recent (tritium-bearing) groundwater found in the surroundings of the southern recharge area in Sinai are characterized by much higher $\delta^{18}O$ and δ^2H values (Gat and Issar, 1974; Tantawi et al., 1998; Yousif et al., 2020).

A similar depleted isotope composition was also encountered in the carbonate aquifer at the western margins of the SAV, in the Gerofit down-faulted block (wells 12 and 13 in Fig. 1c). Previous studies have suggested that the local hydrogeological conditions allow for lateral flow from the sandstone aquifer eastwards into the carbonate aquifer through a series of normal faults (Fig. 2a; Naor et al., 2004). However, a notable ^{81}Kr age difference of 120–150 kyr is observed between the sandstone aquifer's old groundwater in the southern Negev (Shizafon) and the much younger groundwater in the Gerofit Block (Fig. 3c). Thus, the younger ^{81}Kr ages may provide unprecedented evidence for another ^{18}O and ^2H depleted flow component (Group III in Fig. 4) that arrives at the SAV from the west. Further evidence for the presence of such a younger and isotopically depleted groundwater component is encountered 30 km southward in the alluvial aquifer (well #21; 120 kyr; Fig. 4 inset), where the addition of a small amount of brine seems to barely affect the water stable isotope composition.

Within the SAV, isotopically depleted groundwater from the west appears to mix with younger, isotopically enriched groundwater components originating from the east. Such mixing is reflected in the sandstone aquifer's isotope compositions (Fig. 4). The presence of a younger, fresher, and ^{18}O-enriched groundwater component in the NSA is most notable at the northern tip of the SAV (Fig. 5a and b). Interestingly, the isotopic composition of this younger (< 100 kyr) eastern component, which is also reflected in a nearby well that taps the alluvial aquifer (well #11), falls closer to the eastern Mediterranean meteoric water line (Group II in Fig. 4). Furthermore, the relatively low ^{81}Kr age and high $\delta^{18}O$ and δ^2H values for this group resemble the signature of the sandstone aquifer in the northern Negev (Fig. 4), approximately 100 km away, where dominant groundwater recharge by MC (Mediterranean Cyclone) synoptic-scale system was proposed to occur during the LGP (Ram et al., 2020; Yokochi et al., 2019).

The impact of another young (< 50 kyr), fresh, and ^{18}O-enriched groundwater component originating from the east is identified in the carbonate aquifer in the northern part of the SAV (Fig. 5a and b). The latter component (Group I) is distinct in its somewhat lower δ^2H and d_{ex} values compared to that of Group II (Fig. 4). This dissimilar isotope signature suggests groundwater recharge under a different climate regime, namely different dynamics among the possible synoptic-scale systems that transport moisture toward the basin (see further discussion in Section 5.3). Interestingly, the stable isotope composition and young ^{81}Kr age characterizing Group I is quite similar to those observed further southeast in the nearby Disi Aquifer (Fig. 4), where radiocarbon ages of ca. 15–30 kyr were computed (Bajjali and Abu-Jaber, 2001; Vengosh et al., 2010). This indicates that similar synoptic-scale systems were active during the late Pleistocene east of the SAV (the Edom Mountains) and ~100 km further south over the Disi recharge areas in southern Jordan and northwestern Saudi-Arabia (e.g., Charalambous, 2016; El-Naser and Gedeon, 1996).

5.2. *Delineating paleo-recharge components using dissolved noble gases*

The measured dissolved noble gas concentrations (Sup. Table A.2) and the interpreted ΔNe and NGT values)Table 1) enable to further characterize and distinguish between the different groundwater components that reach the SAV from the west (groups III and IV) and east (groups I and II). The old groundwater component (Group IV) is characterized by the highest ΔNe values and Kr/Xe ratios (Fig. 6a). These characteristics were attributed to increased air entrapment and dissolution associated with a rising water table (Ram et al., 2022). In contrast, much lower ΔNe values and Kr/Xe ratios characterize the two young groundwater components (groups I and II; Fig. 6a). Notably, the young groundwater component with the highest d_{ex} signature (Group II) records the lowest recharge temperature of ca. 15 °C (Fig. 6b and c). This recorded NGT is 10–15 °C lower than that of the old groundwater arriving at the SAV from the west (Ram et al., 2022) and highlights the impact of a "cold" last glacial recharge component that entered the northern part of the SAV from the east.

Ideally, the computed NGT represents the ambient soil temperature at the water table at the time of recharge (e.g., Aeschbach-Hertig and Solomon, 2013). In deep groundwater systems such as the sandstone aquifer, for which the current water table is found at a considerable depth below the recharge area (ca. 500–700 m; Issar et al., 1972; JICA, 1999; Ram et al., 2022), the water table temperature is expected to be significantly warmer than the mean annual surface temperature (MAST) due to the geothermal gradient. The computed NGTs for the sandstone aquifer's old groundwater (Group IV) were assessed to be 5–10 °C higher than the current (interglacial) MAST (Ram et al., 2022). Taking into account the local geothermal gradient of ca. 20 °C/km (Abdel Zaher et al., 2014), and considering that paleo-recharge might have taken place under a colder climate (Yokochi et al., 2019), the computed NGTs indicate water table depths of hundreds of meters in the southern recharge area in Sinai, even in times of major groundwater recharge and large-scale water table rise (Ram et al., 2022). In contrast, the NGT signal of the eastern, much younger flow component (Group II) is 10–14 °C colder than the current estimated MAST at the rift valley

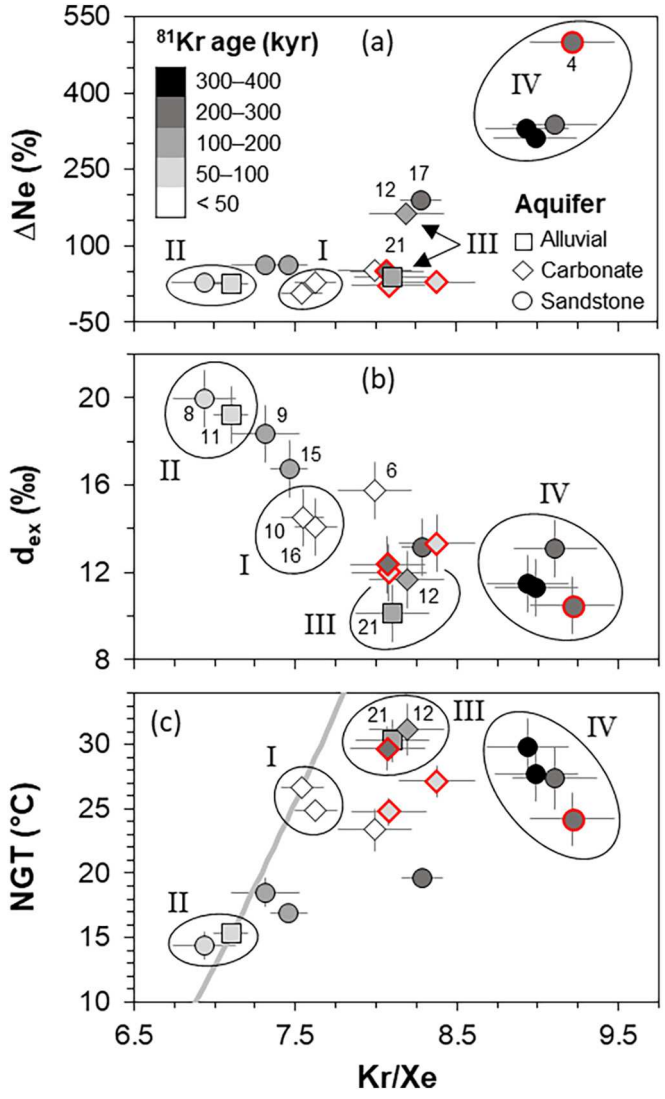

Fig. 6. Measured Kr/Xe ratios in the studied aquifers versus (a) excess Ne (ΔNe) content, (b) d_{ex} values, and (c) noble gas temperatures (NGTs). A red outline marks samples from the southern Negev, and a grey line in subfigure (c) demonstrates the solubility equilibrium Kr/Xe ratio at a given temperature using Jenkins et al. (2019) solubilities. ΔNe errors, as well as NGT errors for some of the samples, are smaller than the symbol size. Kr/Xe error bars represent a propagation of the measurement uncertainties. The marked four clusters (ellipses; groups I–IV) are correlative to those that appear in Fig. 4.

margins (Supplementary Note B.2), where past (and modern) recharge has been proposed to take place (e.g., Adar et al., 1992; Rosenthal et al., 1990). We argue that groundwater recharge during the LGP provides only a partial explanation for the observed low NGT, as a mean cooling of six degrees Celsius was estimated for low-to-mid latitude regions during the Last Glacial Maximum (Seltzer et al., 2021), including a record of ~6.5 °C cooling in the Middle East over this timeframe (Weyhenmeyer et al., 2000). Thus, mountain-block recharge (MBR; e.g., Markovich et al., 2019), i.e., infiltration at the elevated Edom Mountains (Fig. 1b), where lower temperature prevails (Supplementary Note B.2), seems to be an additional factor. MBR by occasional floods at higher elevations and consequent groundwater flow downstream toward the SAV might be feasible in the northern part of the SAV (Gharandal area; Fig. 1b), where the rift's alluvial sediments are in direct contact with Paleozoic and Mesozoic rock formations that outcrops upstream in the mountains, but not further south, where the uplifted basement rocks potentially serve as a hydrological barrier (Fig. 1b).

The other young (< 50 kyr) groundwater component that arrives at the SAV from the east (Group I) is distinct from Group II in the slightly higher Kr/Xe ratio and the much higher computed recharge temperature of ca. 25.5 °C (Fig. 6c). In fact, this recorded NGT is still at the lower range of the current estimated MAST over the SAV (25–29 °C; Supplementary Note B.2). The MAST-NGT gap is even more prominent if considering groundwater recharge through the thick (hundred-m-order) alluvial fans' unsaturated zone (Makhlouf et al., 2010; Radulovic et al., 2020), which is expected to result in surplus geothermal heating of a few °C at the water table depth. Thus, we suggest that the computed NGT for this groundwater component aligns with the scenario of recharge at the eastern margins of the SAV (Adar et al., 1992; Radulovic et al., 2020; Rosenthal et al., 1990) under a colder climate than the present.

High recharge temperatures of ca. 25—30 °C were computed for the carbonate aquifer in the southern Negev (diamonds with a red outline in Fig. 6c). This NGT range is at the upper range and above the estimated current MAST of 21—25 °C (Supplementary note B.2) over the carbonate aquifer's outcrops scattered in the southern Negev and south-central Sinai (Fig. 1a), supporting recharge through a thick (hundreds-of-m order) unsaturated zone and consequent geothermal heating, as in the case of the underlying sandstone aquifer. Despite the similar NGT range, we note that the ΔNe values in the carbonate aquifer over the southern Negev groundwater are much lower than in the underlying aquifer in the southern Negev (Fig. 6a) and upstream in Sinai (Abouelmagd et al., 2014). This considerable gap could result from less efficient air-bubble traps in the fractured carbonate rocks compared to the characteristic sets of fining-upward sediments, from coarse sands to clays. The latter geological settings seem to enhance the air-bubble entrapment and dissolution process during periods of rising water table in the sandstone aquifer (Ram et al., 2022).

The potential utility of the ΔNe signal as a hydrogeological tracer for tracing the origin of groundwater is illustrated in the Gerofit Block (well #12). The ΔNe value in this location is more than three times higher than in any other well that taps the carbonate aquifer (Fig. 6a), and the NGT is also elevated (31 ± 2 °C). This supports groundwater flow from another, probably deeper rock formation into the carbonate aquifer through the adjacent fault (Fig. 2a), with either the Kurnub or the underlying Yam-Suf groups sandstone aquifers serving as plausible sources (Fig. 2a). The high ΔNe, low d_{ex}, and high NGT values in the Gerofit Block are all compatible with groundwater recharge over the southern recharge area in Sinai, and the relatively young ^{81}Kr ages (ca. 150 kyr) may reflect the existence of faster flow trajectories between the southern recharge area and the SAV. Such faster flow routes could also explain the finding of young and isotopically depleted groundwater further south, in the Timna Dome area (well #21; ~120 kyr; Fig. 3a), where the Kr/Xe ratio is very similar to that in the Gerofit Block and the computed NGT is also high (Fig. 6c). A significant gap was obtained in the ΔNe values between the Gerofit Block and the Timna Dome groundwater (well 12 versus 21; Fig. 6a), which cannot be explained at this point. Albeit the different ΔNe signal, we propose that the impact of a similar recharge component is reflected in the ^{81}Kr, noble gas, and water isotope signatures in these two regions (Group III; Fig. 6).

5.3. *Integration of findings with paleo-hydroclimate records*

Regional aquifers are commonly characterized by spatially extended recharge areas. Moreover, surface water could be driven toward the recharge zone from far-away floods. Therefore, and in contrast to the widely used high resolution, time- and site-specific speleothem hydroclimate archive, regional aquifers serve as temporal and spatial integral in a way that short-term climatic variations are smoothed out (e.g., Stute and Schlosser, 1993). Yet, the groundwater archive has the capability to preserve changes in the long-term regional water budget (e.g., Ram et al., 2022; Seltzer et al., 2019), including times when precipitation amounts are below the proposed speleothem deposition threshold (Vaks et al., 2010). For instance, the carbonate aquifer's relatively young ^{81}Kr

ages in the southern Negev provide evidence for significant groundwater recharge in this region over the Late Pleistocene despite the lack of speleothem deposition in the region over this timeframe (Fig. 7a and b). A major advantage of using groundwater as an archive is the capability to preserve the isotope composition of the infiltrating water, including both ^{2}H and ^{18}O relative abundance. In the studied aquifers, near-surface evaporation during ponding, which can lead to enrichment in the heavier isotopes, is expected to only minorly affect the isotope composition of the infiltrating water (e.g., Gat, 1996; Gat and Galai, 1982). This derives from the fast and focused groundwater recharge by major floods that characterize these aquifers. Therefore, the groundwater record enables the examination of the paleo precipitation history through the computed d_{ex} values. The valuable d_{ex} information of the infiltrating water could theoretically also be extracted from speleothem fluid inclusions. However, obtaining a fluid inclusion isotope record is difficult, especially in an arid desert environment, and to date, fluid inclusions over the region have only been studied in the wetter northern parts of Israel (e.g., Affek et al., 2008; Matthews et al., 2021).

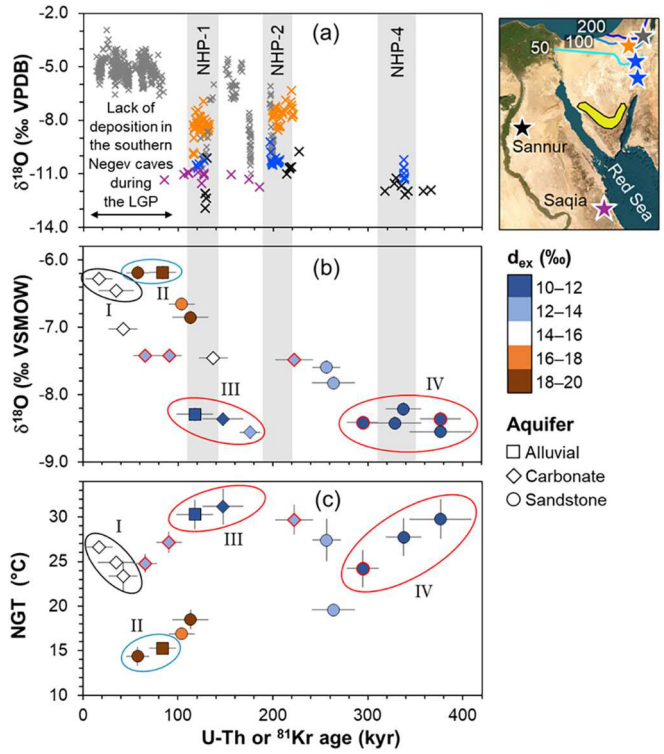

Fig. 7. (a) The speleothem hydroclimate archive, including U—Th ages and $\delta^{18}O$ values (presented in conventional Pee Dee Belemnite units), in caves from the Negev desert (Vaks et al., 2010, 2007, 2006) and the Eastern Desert of Egypt (El-Shenawy et al., 2018; Henselowsky et al., 2021). Cave locations are shown on the map (stars), including (from north to south): Zavoa (northern Negev), Ashalim (central Negev), Ma'ale-ha-Meyshar and Shizafon (southern Negev), Sannur and Saqia (Eastern Desert). (b) ^{81}Kr ages and $\delta^{18}O$ values in the southern Negev (red outlines) and the southern Arava Valley groundwaters. (c) Computed noble gas recharge temperature (NGT) in the studied aquifers. The marked four clusters (ellipses; groups I–IV) are correlative to those from Figs. 4 and 6. The colors of the ellipses are correlative to those of the groundwater components shown in Fig. 8b. Also shown on the map are isohyets (colored as in Fig. 1a) and the southern recharge area location (yellow polygon). Grey shades in subfigures a and b mark wetter episodes in the southern Negev (originally termed Negev Humid Periods; NHPs) as proposed by Vaks et al. (2010). Note the overlap in the timing of ^{18}O-depleted speleothem deposition in the southern Negev and the Eastern Desert. These wetter periods seem to be at least partially reflected in the ^{18}O-depleted groundwater recharged through the southern outcrops in Sinai, i.e., between the cave locations. Satellite imagery source: Earthstar Geographics (powered by Esri).

Groundwater mixing, which may occur either naturally (e.g., hydrodynamic dispersion or cross-formational flow in fault zones) or artificially (e.g., pumping from various water-bearing formations), complicates the usage of aquifers as a long-term (100-kyr-timescale) climatic archive. Even for a simple 1-D aquifer with a single recharge area, longitudinal dispersion will likely smooth climatic tracer signals (including noble gases, water isotopes, etc.) over longer timescales (Stute and Schlosser, 1993). However, our current and former studies (Ram et al., 2022; Yokochi et al., 2019) provide evidence that large-scale aquifers in arid regions can preserve long-term climatic signals. We hypothesize that the transient nature of groundwater recharge in this arid region (and others), with major pulse-like recharge events during short wet episodes (Vaks et al., 2010, 2007) followed by prolonged dry periods (Amit et al., 2011, 2006) with minimal recharge, may lead to the formation of distinct "individual" groundwater parcels. These parcels represent a low-frequency signal that is maintained over long flow and time scales (e.g., Petersen et al., 2014). The groundwater flow in such a desert aquifer system takes place under changing hydraulic gradients (Schulz et al., 2017), with a gradual water table and discharge rate decline during drier periods (e.g., Issar, 1979; Issar et al., 1972).

Groundwater mixing is clearly reflected in the current study in the sandstone aquifer's water isotope composition (Fig. 4), demonstrating a differential contribution of the various flow components along the SAV. Mixing could also explain the overall scatter in the computed ^{81}Kr ages over the past 400 kyr (Fig. 7b). Therefore, we stress that ^{81}Kr-$\delta^{18}O$-d_{ex} combination in an individual well could not be considered a stand-alone record of a "single" paleorecharge event, especially in the studied production wells with tens-of-m-long screened intervals (Fig. 2), for which mixing among various water-bearing formations is plausible. This underscores the need to integrate data from multiple wells and apply a wide range of atmospheric-derived tracers to characterize groundwater flow components. Specifically, the application of the inert noble gases provided crucial tiers in the current study for distinguishing groundwater of different origins, including differences in the measured Kr/Xe ratios (Fig. 6) and computed recharge temperatures (Fig. 7c).

In the following subsections, we synthesize the groundwater findings with other near-terrestrial records to enhance the understanding of the regional hydroclimate archive.

5.3.1. *Southern Negev and Sinai 100–400 kyr records*

To the west of the SAV, three wetter periods were previously proposed based on cave deposits from the southern Negev. These short-term wet episodes, referred to as "Negev Humid Periods" (NHP) by Vaks et al. (2010), occurred between ca. 350—310, 220—190, and 140—110 kyr (NHP-4, 2 and 1, respectively). The southern Negev speleothems are characterized by low $\delta^{18}O$ values (Fig. 7a). Based on the speleothems' frequency and thickness, it was proposed that NHP-1, which corresponds to the penultimate Interglacial (Marine Isotope Stage 5), was the wettest among these more pluvial periods (Vaks et al., 2010). The impact of this wetter episode is also evidenced further south in the Red Sea marine record through the fossil coral reef (Lazar and Stein, 2011; Yehudai et al., 2017) and sediment Nd isotope composition (Hartman et al., 2020) records, both indicators for a larger contribution of freshwater into the sea. The timing of this identified wetter interglacial episode during which ^{18}O-depleted calcite was deposited in the southern Negev caves partially overlaps with the relatively young and ^{18}O-depleted groundwater component (Group III in Fig. 7b) that flows toward the SAV from the west (Sinai Peninsula). Some overlap also exists between the ^{18}O-depleted cave deposits during NHP-4 and the old, ^{18}O-depleted groundwater (Group IV) recharged through the southern outcrops in Sinai, 200 km southwestwards (Fig. 7). In fact, the proposed agreement among the groundwater and speleothem records extends further southwest: Speleothems from the Eastern Desert of Egypt (Sannur and Saqia caves) present ^{18}O-depleted calcite precipitation contemporary (although with a larger temporal scatter that also covers some glacial epochs) to that in the southern Negev during NHP-1 and

NHP-4 (Fig. 7a; El-shenawy et al., 2018; Henselowsky et al., 2021).

Despite the large ^{81}Kr age range and uncertainties which are hidden in groups III and IV groundwater clusters, the observed partial agreement with near-surface records may propose a synchronization of ^{18}O-depleted wet episodes over the southern Negev and southern Sinai during the mid-to-late Pleistocene. Furthermore, the identified similar δ^{18}O and d_{ex} signature among the very old and the somewhat younger groundwater components (groups III and IV; Fig. 7b) provides first and unique groundwater-based evidence that comparable hydroclimatic conditions occurred intermittently over the past 400 kyr. The water isotope signature stands in line with the hypothesis of dominant moisture transportation from lower latitudes by, e.g., tropical plumes, which are capable of transporting and producing high-magnitude floods over extended areas of the arid southeastern Mediterranean (Armon et al., 2018; Rubin et al., 2007; Waldmann et al., 2010; Yokochi et al., 2019). Thus, the combined groundwater and speleothem records may serve as an indication of the regional nature of past pluvial episodes in the southeastern Mediterranean during which significant groundwater recharge and major water table rise (Ram et al., 2022) have taken place.

5.3.2. Edom Mountains' surroundings < 100 kyr records

To the east of the SAV, investigations of fluvial-lacustrine sediments at the Gharandal streambed (wadi), situated near the foothills of the Edom Mountains (Fig. 1b), indicate the occurrence of two wetter episodes during the Late Pleistocene. Optically stimulated luminescence (OSL) dating reveals ages of 112 ± 9 and 32 ± 4 kyr (Ginat et al., 2018). The younger event is further supported by the radiocarbon age of 25–38 kyr of buried organic material collected from the upper part of the Gharandal's lacustrine record (Mischke et al., 2017). While the Gharandal streambed drains a relatively small catchment area at the steep western flanks of the Edom Mountains, the Al Jafr depression, located ca. 100 km to the east, drains a large portion of the eastern flanks of the ridge. Paleo- wetland sediments and archeological findings from this site record more pluvial conditions around 83 (Macumber, 2001) and 16—42 kyr ago (Davies, 2005; Ginat et al., 2018; Mischke et al., 2015); the latter episode overlaps the western flank (Gharandal) record. Thus, intermittent wetter and drier episodes over southern Jordan during the past 100 kyr, including a wet episode(s) over the past few tens of thousands of years, are reflected in these terrestrial records. Our groundwater record now enhances the regional hydroclimate archive with additional insights: The young ^{81}Kr groundwater ages (< 50 kyr) in the carbonate aquifer and the slightly older ages (50—100 kyr) in the sandstone and the alluvial aquifers in the northern parts of the SAV (groups I and II, respectively) confirm substantial recharge over the Edom Mountains during the LGP. Furthermore, the different d_{ex} and NGT signatures of groups I and II (Fig. 6b and c) demonstrate distinct hydroclimatic conditions (synoptic-scale system dynamics) and locations (altitude) of the paleo-recharge.

A remarkable finding is the overlap in the stable isotope composition of Group II and the northern Negev Last Glacial groundwaters (Fig. 4). This similarity, and specifically, the characteristic high d_{ex} value which resembles that of Eastern Mediterranean meteoric waters (Fig. 4), suggests a higher frequency and/or intensity of MCs that traveled further inland and southward during this timeframe, resulting in increased precipitation and significant groundwater replenishment which have taken place in areas surrounding the Edom Mountains. A wet last glacial was also inferred from speleothem records from the northern Negev (Fig. 7a) but not in caves found further south (Vaks et al., 2018, 2006). Even under the current climate, the Edom Mountains receive somewhat higher precipitation amounts compared to the hyperarid southern Negev that lies to the west (see isohyets in Fig. 1a), including MCs that almost entirely "skip" the central and southern Negev but do precipitate over the elevated mountains (e.g., Armon et al., 2019; Enzel et al., 2008). The isotope composition of current rainwater from the northern part of the Edom Mountains (Shoubak weather station; Fig. 1a) is compatible with an eastern Mediterranean moisture source (Fig. 4) and is not very different from those observed in the wetter parts of Jordan, where MCs are dominant (Armon et al., 2019; Bajjali, 2012).

5.4. Hydroclimatic groundwater archive insights

Overall, and despite the potential complexity resulting from mixing processes, we propose that the groundwater paleo-hydroclimate record presented and discussed in the frame of the current study reflects the impact of at least four recharge components (groups I–IV). The geochemical signatures that characterize these components demonstrate groundwater recharge under distinct climatic conditions at different times, taking place over various recharge areas. The two older components (groups III and IV) are characterized by the most depleted water stable isotope composition, with d_{ex} values that are in accordance with dominant moisture transportation from the eastern Atlantic (West Africa) toward the region (Fig. 8a and b, red arrows). These groundwater components, which flow toward the SAV from the west (Fig. 8b), also carry the highest amount of dissolved excess air (ΔNe) and a high NGT signal. The first serves as evidence for major water table rises during wet

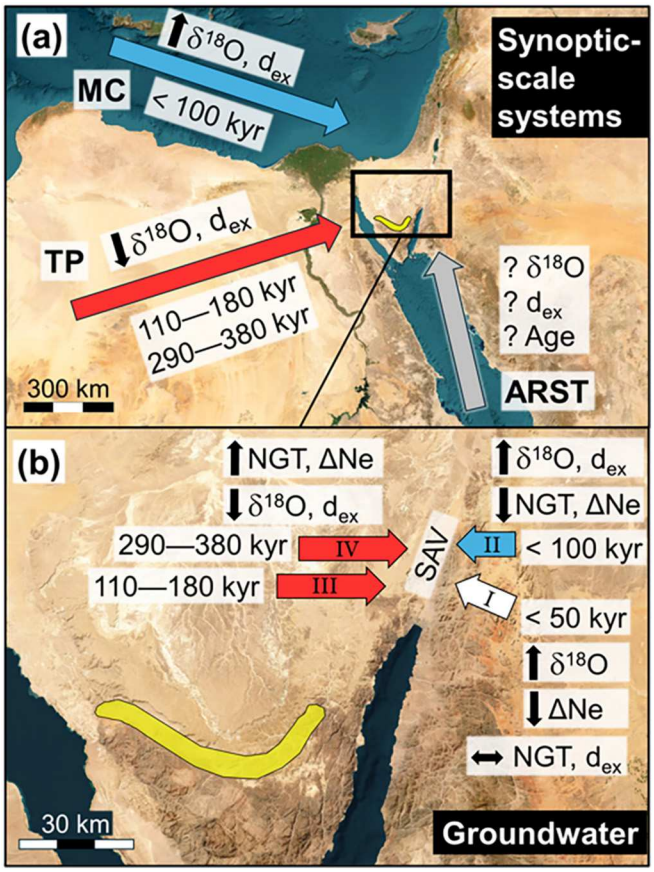

Fig. 8. A conceptual model of the pathways of the SAV groundwater recharge, showing (a) the paths of different synoptic-scale systems that potentially transport moisture to the arid southeastern Mediterranean, and (b) the groundwater record, with different flow components (arrows with group annotations) that arrives at the SAV from both sides of the rift. Arrow colors in Subfigure b correlate to those in Subfigure a. Time intervals denote the observed ^{81}Kr age range of the groundwaters (without margins). δ^{18}O and d_{ex} refer to the water stable isotope composition, NGT is the noble gas-based computed recharge temperature, and ΔNe depicts the amount of "excess air" dissolved in the groundwater. Note the different ^{81}Kr age-δ^{18}O-d_{ex}-NGT-ΔNe combinations of the various components. MCs, TP, and ARST are Mediterranean cyclone, tropical plume, and active Red Sea trough synoptic-scale systems. A yellow polygon denotes the location of the southern recharge area in Sinai. Satellite imagery source: Earthstar Geographics (powered by Esri).

episodes in the hyperarid region, and the latter is explained by a great water table depth (hundreds of m) below the recharge area and consequent geothermal heating (Fig. 8b). The identified two other younger (< 100 kyr) components entered the SAV from the east (Fig. 8b) and differ from one another by their d_{ex} and NGT signatures, which suggests a different recharge history: A dominant transportation of moisture by MCs (Fig. 8a) toward the Edom Mountains and groundwater recharge at higher elevation during the LGP is reflected in the high d_{ex} and low NGT for one component (Groups II). For the other component (Group I), with an intermediate d_{ex} value (ca. 14 ‰), recharge at the SAV eastern margins (the mountain foothills) seems reasonable, whereas the nature of paleo-precipitation (i.e., the relative contribution from the various plausible synoptic-scale systems and moisture sources) remains obscure. Future detailed spatial mapping upstream of the regional aquifers in Sinai (Egypt) and east of the SAV (southern Jordan) utilizing a similar ensemble of geochemical tracers holds potential for further deconvolution of the distinct flow components. This, in turn, will provide an opportunity for a more quantitative estimation of the relative contribution of older and younger groundwater components (e.g., van Rooyen et al., 2022).

6. Summary and conclusions

Old groundwater, recharged during past wetter episodes, is prevalent globally in deep regional aquifers in low- to mid-latitude arid environments. Our study demonstrates how long-term (100-kyr-timescale) paleo-hydroclimate signals, which are preserved in such deep desert aquifers, can be reconstructed by interpreting multiple atmosphere-derived tracers, including cosmogenic radioisotopes, water stable isotopes, and dissolved noble gas compositions. The resultant groundwater proxy record re-affirms and expands our paleo-hydroclimatic knowledge beyond other, terrestrial-based records, with direct indications for periods with a significant contribution to the regional water budget which occurred both to the west (Sinai and Negev deserts) and east (Edom Mountains) of the Arava Valley over the past 400 kyr. The varying hydroclimates that prevailed over this timeframe are highlighted by the d_{ex} variations, and the different noble gas signals provided evidence for additional groundwater sources with different recharge histories that were mixed into the main system along the flow path.

A partial overlap was observed between the timing of ^{18}O-depleted groundwater recharge, as reflected in the groundwater record, and ^{18}O-depleted calcite deposition in caves from the hyperarid region. We propose that these two archives, which provide different hydroclimate evidence in terms of resolution, spatial extent, and intensity, complement each other and together provide a more complete hydroclimate record. Specifically, the information on deuterium and d_{ex} values, which are missing in the speleothem record, provides an important insight into the moisture source origin of past wetter episodes. The partial overlap and the similar $\delta^{18}O$ pattern among the two records are encouraging for the use of groundwater as a climatic archive at the 100-kyr timescale. In addition, the combined evidence from these two paleo-hydroclimate records sharpens our understanding regarding the nature of major groundwater recharge processes in this arid region, which occurs episodically (i.e., focused over certain more pluvial times) rather than continuously (e.g., Petersen et al., 2014).

Distinguishing and quantifying deep groundwater components is necessary for a paleo-hydroclimate reconstruction and, not of less importance, for sustainable water resource management of multiple cross-bordering aquifers. Such a hydrogeological and geochemical study becomes even more critical as climate change may cause a differential impact on the availability of natural groundwater resources in arid environments such as the Middle East, which is among the regions that suffer the most from water scarcity worldwide. Utilization of similar methodologies and research tools in other desert aquifers, such as the deep groundwater systems of North Africa and the Arabian Peninsula, has the potential to further unravel the regional hydroclimatic history of arid basins, particularly in locations presently lacking terrestrial paleo-climate records.

Funding

This work was funded by the Ben-Gurion University-Argonne National Laboratory-University of Chicago Collaboration Program; the United States-Israel Binational Science Foundation (Grant No. 2014351); the Israel Science Foundation (ISF) and the National Natural Science Foundation of China joint program (No. 41961144027); the Israel Water Authority, Ministry of Energy (No. 4501284811); and the ISF research grant (No. 2185/22). Work at the Argonne National Laboratory was supported by the U.S. Department of Energy, Office of Science, under contract DE-AC02-06CH11357. In addition, the research has been supported by grants given to the first author of this work by the Ministry of Science and Technology of Israel and the Minerva Stiftung Gesellschaft fuer die Forschung mbH. MA was funded by the Swiss National Science Foundation (No. TMPFP2_216989), and AMS was supported by the US National Science Foundation award (No. HS-2238641).

CRediT authorship contribution statement

Roi Ram: Writing – review & editing, Writing – original draft, Visualization, Investigation, Formal analysis, Data curation, Conceptualization. **Eilon M. Adar:** Writing – review & editing, Supervision, Resources, Project administration, Investigation, Funding acquisition, Data curation, Conceptualization. **Yoseph Yechieli:** Writing – review & editing, Supervision, Resources, Project administration, Investigation, Funding acquisition, Data curation, Conceptualization. **Reika Yokochi:** Resources, Methodology, Investigation, Funding acquisition, Formal analysis, Data curation, Conceptualization. **Werner Aeschbach:** Writing – review & editing, Validation, Software, Resources, Methodology, Investigation. **Moshe Armon:** Writing – review & editing, Visualization, Investigation, Conceptualization. **D. Kip Solomon:** Writing – review & editing, Validation, Methodology, Investigation, Formal analysis, Data curation. **Roland Purtschert:** Writing – review & editing, Visualization, Resources, Methodology, Investigation, Formal analysis, Data curation, Conceptualization. **Alan M. Seltzer:** Writing – review & editing, Investigation, Data curation, Conceptualization. **Kerstin L. Urbach:** Writing – review & editing, Validation, Formal analysis, Data curation. **Michael Bishof:** Writing – review & editing, Methodology, Formal analysis. **Peter Mueller:** Writing – review & editing, Resources, Methodology, Funding acquisition, Formal analysis, Data curation. **Jake C. Zappala:** Writing – review & editing, Investigation, Formal analysis, Data curation, Conceptualization. **Wei Jiang:** Writing – review & editing, Resources, Methodology, Funding acquisition, Formal analysis, Data curation. **Zheng-Tian Lu:** Writing – review & editing, Resources, Methodology, Funding acquisition, Formal analysis, Data curation, Conceptualization. **Itay J. Reznik:** Writing – review & editing, Visualization, Supervision, Resources, Project administration, Investigation, Funding acquisition, Formal analysis, Data curation, Conceptualization.

Declaration of competing interest

The authors declare that they have no known competing financial interests or personal relationships that could have appeared to influence the work reported in this paper.

Data availability

All geochemical and isotope data on which the study is based are provided in the paper (Table 1) and the supplementary files (Tables A.1 to A.4).

Acknowledgments

Dedicated to our dear friend and colleague, Reika Yokochi, whose open mind and fresh perspectives significantly contributed to our understanding of hydrological systems and processes. We thank the Israel Water Authority and the Mekorot National Water Company for providing access to the sampled wells. Lab staff of the Geological Survey of Israel (GSI) and the Zuckerberg Institute for Water Research are thanked for their precise analytical work. We thank Dr. Avihu Burg (GSI), Arik Zurieli (Israel Water Authority), and Dr. Joseph Guttman (Mekorot) for sharing their knowledge regarding the Southern Arava hydrogeological system. Dr. Burg is also thanked for a constructive review of an earlier version of the manuscript. We would also like to express our sincere gratitude to Dr. Edith Engelhardt (Heidelberg University) and Wil Mace (University of Utah) for their great help with the noble gas measurement and data acquisition efforts. The three anonymous reviewers are greatly acknowledged for their constructive comments which improved the paper significantly.

Appendix A. Supplementary data

Supplementary data to this article can be found online at https://doi.org/10.1016/j.scitotenv.2024.175737.

References

Abdel Zaher, M., El Nuby, M., Ghamry, E., Mansour, K., Saadi, N.M., Atef, H., 2014. Geothermal studies in oilfield districts of eastern margin of the Gulf of Suez. Egypt. NRIAG J. Astron. Geophys. 3, 62–69. https://doi.org/10.1016/j.nrjag.2014.04.002.

Abouelmagd, A., Sultan, M., Milewski, A., Kehew, A.E., Sturchio, N.C., Soliman, F., Krishnamurthy, R.V., Cutrim, E., 2012. Toward a better understanding of palaeoclimatic regimes that recharged the fossil aquifers in North Africa: inferences from stable isotope and remote sensing data. Palaeogeogr. Palaeoclimatol. Palaeoecol. 329–330, 137–149. https://doi.org/10.1016/j.palaeo.2012.02.024.

Abouelmagd, A., Sultan, M., Sturchio, N.C., Soliman, F., Rashed, M., Ahmed, M., Kehew, A.E., Milewski, A., Chouinard, K., 2014. Paleoclimate record in the Nubian sandstone aquifer, Sinai peninsula. Egypt. Quat. Res. 81, 158–167.

Adar, E.M., Rosenthal, E., Issar, A.S., Batelaan, O., 1992. Quantitative assessment of the flow pattern in the southern Arava Valley (Israel) by environmental tracers and a mixing cell model. J. Hydrol. 136, 333–352.

Aeschbach-Hertig, W., 2014. Radiokrypton dating finally takes off. Proc. Natl. Acad. Sci. 111, 6856–6857.

Aeschbach-Hertig, W., Solomon, D.K., 2013. Noble gas thermometry in groundwater hydrology. In: Burnard, P.G. (Ed.), The Noble Gases as Geochemical Tracers. Springer, Berlin, Heidelberg, pp. 81–122. https://doi.org/10.1007/978-3-642-28836-4_5.

Aeschbach-Hertig, W., Peeters, F., Beyerle, U., Kipfer, R., 2000. Palaeotemperature reconstruction from noble gases in ground water taking into account equilibration with entrapped air. Nature 405, 1040–1044.

Aeschbach-Hertig, W., Beyerle, U., Holocher, J., Peeters, F., Kipfer, R., 2002. Excess air in ground water as a potential indicator of past environmental changes. In: International Atomic Energy Agency (Ed.), Study of Environmental Change Using Isotope Techniques, Vienna, C&S Papers Series, vol. 13, ISBN 92-0-116402-5, pp. 174–183.

Affek, H.P., Bar-Matthews, M., Ayalon, A., Matthews, A., Eiler, J.M., 2008. Glacial/interglacial temperature variations in Soreq cave speleothems as recorded by 'clumped isotope' thermometry. Geochim. Cosmochim. Acta 72, 5351–5360. https://doi.org/10.1016/j.gca.2008.06.031.

Amit, R., Enzel, Y., Sharon, D., 2006. Permanent quaternary hyperaridity in the Negev, Israel, resulting from regional tectonics blocking Mediterranean frontal systems. Geology 34, 509–512.

Amit, R., Simhai, O., Ayalon, A., Enzel, Y., Matmon, A., Crouvi, O., Porat, N., McDonald, E., 2011. Transition from arid to hyper-arid environment in the southern Levant deserts as recorded by early Pleistocene cummulic Aridisols. Quat. Sci. Rev. 30, 312–323. https://doi.org/10.1016/j.quascirev.2010.11.007.

Arad, A., Kafri, U., 1980. Hydrogeological interrelationship between the Judea group and the Nubian sandstone aquifers in Sinai and the Negev. Isr. J. Earth Sci. 29, 67–72.

Armon, M., Dente, E., Smith, J.A., Enzel, Y., Morin, E., 2018. Synoptic-scale control over modern rainfall and flood patterns in the Levant drylands with implications for past climates. J. Hydrometeorol. 19, 1077–1096. https://doi.org/10.1175/JHM-D-18-0013.1.

Armon, M., Morin, E., Enzel, Y., 2019. Overview of modern atmospheric patterns controlling rainfall and floods into the Dead Sea: implications for the lake's sedimentology and paleohydrology. Quat. Sci. Rev. 216, 58–73. https://doi.org/10.1016/j.quascirev.2019.06.005.

Atencio, B., Ram, R., Burg, A., Yokochi, R., Yechieli, Y., Purtschert, R., Lu, Z.-T., Jiang, W., Ronen, Z., Adar, E.M., 2024. Investigating the enigma of an irregular groundwater age pattern in a confined, presumed "fossil" complex aquifer through mixing cell flow modeling. J. Hydrol. 630, 130631 https://doi.org/10.1016/j.jhydrol.2024.130631.

Bajjali, W., 2012. Spatial variability of environmental isotope and chemical content of precipitation in Jordan and evidence of slight change in climate. Appl Water Sci 2, 271–283. https://doi.org/10.1007/s13201-012-0046-1.

Bajjali, W., Abu-Jaber, N., 2001. Climatological signals of the paleogroundwater in Jordan. J. Hydrol. 243, 133–147. https://doi.org/10.1016/S0022-1694(00)00409-1.

Bein, A., Yechieli, Y., Bensabat, J., 2001. Quantifying the groundwater resources of the southern Arava Rift Valley: a confined desert system recharged laterally by external sources. Isr. J. Earth Sci. 50, 217–236.

Bekaert, D.V., Blard, P.-H., Raoult, Y., Pik, R., Kipfer, R., Seltzer, A.M., Legrain, E., Marty, B., 2023. Last glacial maximum cooling of 9 °C in continental Europe from a 40 kyr-long noble gas paleothermometry record. Quat. Sci. Rev. 310, 108123 https://doi.org/10.1016/j.quascirev.2023.108123.

Beyerle, U., Rueedi, J., Leuenberger, M., Aeschbach-Hertig, W., Peeters, F., Kipfer, R., Dodo, A., 2003. Evidence for periods of wetter and cooler climate in the Sahel between 6 and 40 kyr BP derived from groundwater. Geophys. Res. Lett. 30, 1173. https://doi.org/10.1029/2002GL016310.

Burg, A., Zilberbrand, M., Yechieli, Y., 2013. Radiocarbon variability in groundwater in an extremely arid zone - the Arava Valley, Israel. Radiocarbon 55, 963–978.

Charalambous, A.N., 2016. The fossil ram sandstone aquifer of Jordan: hydrogeology, depletion and sustainability. Q. J. Eng. Geol. Hydrogeol. 49, 76–91. https://doi.org/10.1144/qjegh2015-060.

Davies, C.P., 2005. Quaternary paleoenvironments and potential for human exploitation of the Jordan plateau desert interior. Geoarchaeology 20, 379–400. https://doi.org/10.1002/gea.20055.

de Vries, A.J., Tyrlis, E., Edry, D., Krichak, S.O., Steil, B., Lelieveld, J., 2013. Extreme precipitation events in the Middle East: dynamics of the active Red Sea trough. J. Geophys. Res. Atmos. 118, 7087–7108. https://doi.org/10.1002/jgrd.50569.

El-Naser, H., Gedeon, R., 1996. Hydrochemistry and Isotopic Composition of the Nubian Sandstone Aquifers of Disi-Mudawwara Area. South Jordan, International Atomic Energy Agency (IAEA).

El-Shenawy, M.I., Kim, S., Schwarcz, H.P., Asmerom, Y., Polyak, V.J., 2018. Speleothem evidence for the greening of the Sahara and its implications for the early human dispersal out of sub-Saharan Africa. Quat. Sci. Rev. 188, 67–76. https://doi.org/10.1016/j.quascirev.2018.03.016.

Enzel, Y., Amit, R., Dayan, U., Crouvi, O., Kahana, R., Ziv, B., Sharon, D., 2008. The climatic and physiographic controls of the eastern Mediterranean over the late Pleistocene climates in the southern Levant and its neighboring deserts. Glob. Planet. Chang. 60, 165–192. https://doi.org/10.1016/j.gloplacha.2007.02.003.

Eyal, M., Bartov, Y., Shimron, A.E., Bentor, Y.K., 1980. Sinai Geological Map. Scale 1 (500), 000.

Fick, S.E., Hijmans, R.J., 2017. WorldClim 2: new 1-km spatial resolution climate surfaces for global land areas. Int. J. Climatol. 37, 4302–4315. https://doi.org/10.1002/joc.5086.

Fleischer, L., Gafsou, R., 2003. Top Judea Group digital structural map of Israel, the Geophysical Institute of Israel map. Rep 753/312/03, 19 p. and maps.

Fleitmann, D., Burns, S.J., Mangini, A., Mudelsee, M., Kramers, J., Villa, I., Neff, U., Al-Subbary, A.A., Buettner, A., Hippler, D., Matter, A., 2007. Holocene ITCZ and Indian monsoon dynamics recorded in stalagmites from Oman and Yemen (Socotra). Quat. Sci. Rev. 26, 170–188. https://doi.org/10.1016/j.quascirev.2006.04.012.

Gat, J.R., 1996. Oxygen and hydrogen isotopes in the hydrologic cycle. Annu. Rev. Earth Planet. Sci. 24, 225–262.

Gat, J.R., Dansgaard, W., 1972. Stable isotope survey of the fresh water occurrences in Israel and the northern Jordan Rift Valley. J. Hydrol. 16, 177–211. https://doi.org/10.1016/0022-1694(72)90052-2.

Gat, J.R., Galai, A., 1982. Groundwaters of the Arava Valley - an isotopic study of their origin and interrelationships. Isr. J. Earth Sci. 31, 25–38.

Gat, J.R., Issar, A., 1974. Desert isotope hydrology: Water sources of the Sinai Desert. Geochim. Cosmochim. Acta 38, 1117–1131.

Gerber, C., Vaikmae, R., Aeschbach, W., Babre, A., Jiang, W., Leuenberger, M., Lu, Z.T., Mokrik, R., Muller, P., Raidla, V., Saks, T., Waber, H.N., Weissbach, T., Zappala, J.C., Purtschert, R., 2017. Using 81Kr and noble gases to characterize and date groundwater and brines in the Baltic Artesian Basin on the one-million-year timescale. Geochim. Cosmochim. Acta 205, 187–210. https://doi.org/10.1016/j.gca.2017.01.033.

Ginat, H., Opitz, S., Ababneh, L., Faershtein, G., Lazar, M., Porat, N., Mischke, S., 2018. Pliocene-Pleistocene waterbodies and associated deposits in southern Israel and southern Jordan. J. Arid Environ. 148, 14–33. https://doi.org/10.1016/j.jaridenv.2017.09.007.

Goldreich, Y., 2003. The Climate of Israel: Observation, Research and Application. Kluwer Academic Press & Plenum Publishers, New York, NY, p. 270.

Goldreich, Y., Karni, O., 2001. Climate and precipitation regime in the Arava Valley. Israel. Isr. J. Earth Sci. 50, 53–60. https://doi.org/10.1560/1v61-fpgf-y5vk-adag.

Guttman, Y., Burg, A., Lifshitz, Y., Lumelsky, S., Zukerman, H., 1999. Hydrological Model for Estimation of Water Potential in the Arava Aquifers – Final Report. Tahal Company Ltd. Report 6127-d99.201. 52 p. (In Hebrew).

Hartman, A., Torfstein, A., Almogi-Labin, A., 2020. Climate swings in the northern Red Sea over the last 150,000 years from εNd and mg/ca of marine sediments. Quat. Sci. Rev. 231, 106205 https://doi.org/10.1016/j.quascirev.2020.106205.

Henselowsky, F., Eichstädter, R., Schröder-Ritzrau, A., Herwartz, D., Almoazamy, A., Frank, N., Kindermann, K., Bubenzer, O., 2021. Speleothem growth phases in the central Eastern Desert of Egypt reveal enhanced humidity throughout MIS 5. Quat. Int. https://doi.org/10.1016/j.quaint.2021.05.006.

Ingram, R.G.S., Hiscock, K.M., Dennis, P.F., 2007. Noble gas excess air applied to distinguish groundwater recharge conditions. Environ. Sci. Technol. 41, 1949–1955. https://doi.org/10.1021/es061115r.

Issar, A., 1979. The paleohydrology of southern Israel and its influence on the flushing of the Kurnub and 'Arad groups (Lower Cretaceous and Jurassic). J. Hydrol. 44, 289–303.

Issar, A., Bein, A., Michaeli, A., 1972. On the ancient water of the upper Nubian sandstone aquifer in Central Sinai and southern Israel. J. Hydrol. 17, 353–374. https://doi.org/10.1016/0022-1694(72)90092-3.

Jasechko, S., Perrone, D., Befus, K.M., Bayani Cardenas, M., Ferguson, G., Gleeson, T., Luijendijk, E., McDonnell, J.J., Taylor, R.G., Wada, Y., Kirchner, J.W., 2017. Global aquifers dominated by fossil groundwaters but wells vulnerable to modern contamination. Nat. Geosci. 10, 425–430. https://doi.org/10.1038/ngeo2943.

Jenkins, W.J., Lott, D.E., Cahill, K.L., 2019. A determination of atmospheric helium, neon, argon, krypton, and xenon solubility concentrations in water and seawater. Mar. Chem. 211, 94–107. https://doi.org/10.1016/j.marchem.2019.03.007.

Jiang, W., Bailey, K., Lu, Z.T., Mueller, P., O'Connor, T.P., Cheng, C.F., Hu, S.M., Purtschert, R., Sturchio, N.C., Sun, Y.R., Williams, W.D., Yang, G.M., 2012. An atom counter for measuring 81Kr and 85Kr in environmental samples. Geochim. Cosmochim. Acta 91, 1–6.

Jiang, W., Hu, S.-M., Lu, Z.-T., Ritterbusch, F., Yang, G., 2020. Latest development of radiokrypton dating – a tool to find and study paleogroundwater. Quat. Int. 547, 166–171. https://doi.org/10.1016/j.quaint.2019.04.025.

JICA, 1999. South Sinai Groundwater Resources Study in the Arab Republic of Egypt. Japan International Cooperation Agency and Water Resources Research Institute. Pacific Consultants International and Sanyu Consultants Inc Rep, Tokyo.

Jouzel, J., Delaygue, G., Landais, A., Masson-Delmotte, V., Risi, C., Vimeux, F., 2013. Water isotopes as tools to document oceanic sources of precipitation. Water Resour. Res. 49, 7469–7486. https://doi.org/10.1002/2013WR013508.

Jung, M., Aeschbach, W., 2018. A new software tool for the analysis of noble gas data sets from (ground)water. Environ. Model Softw. 103, 120–130. https://doi.org/10.1016/j.envsoft.2018.02.004.

Jung, M., Wieser, M., von Oehsen, A., Aeschbach-Hertig, W., 2013. Properties of the closed-system equilibration model for dissolved noble gases in groundwater. Chem. Geol. 339, 291–300. https://doi.org/10.1016/j.chemgeo.2012.08.006.

Kahana, R., Ziv, B., Enzel, Y., Dayan, U., 2002. Synoptic climatology of major floods in the Negev Desert. Israel. Int. J. Climatol. 22, 867–882. https://doi.org/10.1002/joc.766.

Kroitoru, L., 1980. The Hydrogeology of the Nubian Sandstone in Southern Israel. Thesis, Tel Aviv University (In Hebrew, English abstract), M.Sc.

Kroitoru, L., Kronfeld, J., Ginzburg, A., 1981. The geohydrology of the Gerofit-Ya'alon area. Isr. J. Earth Sci. 30, 24–30.

Kulongoski, J.T., Hilton, D.R., Selaolo, E.T., 2004. Climate variability in the Botswana Kalahari from the late Pleistocene to the present day. Geophys. Res. Lett. 31 (10) https://doi.org/10.1029/2003GL019238.

Kushnir, Y., Dayan, U., Ziv, B., Morin, E., Enzel, Y., 2017. Climate of the Levant: Phenomena and mechanisms. In: Enzel, Y., Bar-Yosef, O. (Eds.), Quaternary of the Levant: Environments, Climate Change, and Humans. Cambridge University Press, pp. 31–44.

Lazar, B., Stein, M., 2011. Freshwater on the route of hominids out of Africa revealed by U-Th in Red Sea corals. Geology 39, 1067–1070. https://doi.org/10.1130/G32257.1.

Leguy, C., Rindsberger, M., Zangwil, A., Issar, A., Gat, J.R., 1983. The relation between the 18O and deuterium contents of rain water in the Negev Desert and air-mass trajectories. Chem. Geol. 41, 205–218. https://doi.org/10.1016/S0009-2541(83)80019-9.

Macumber, P.G., 2001. Evolving landscape and environment in Jordan. In: MacDonald, B., Adams, R., Bienkowski, P. (Eds.), The Archaeology of Jordan. Sheffield Academic Press, pp. 1–30.

Makhlouf, I.M., Amireh, B.S., Abed, A.M., 2010. Sedimentology and morphology of quaternary alluvial fans in Wadi Araba, Southwest Jordan. Jordan J. Earth Environ. Sci. 3, 79–98.

Markovich, K.H., Manning, A.H., Condon, L.E., McIntosh, J.C., 2019. Mountain-Block Recharge: A Review of Current Understanding. Water Resour. Res. 55, 8278–8304. https://doi.org/10.1029/2019WR025676.

Matsumoto, T., Zouari, K., Trabelsi, R., Hillegonds, D., Jiang, W., Lu, Z.T., Mueller, P., Zappala, J.C., Araguás Araguás, L.J., Romeo, N., Agoun, A., 2020. Krypton-81 dating of the deep continental Intercalaire aquifer with implications for chlorine-36 dating. Earth Planet. Sci. Lett. 535, 116120 https://doi.org/10.1016/j.epsl.2020.116120.

Matthews, A., Affek, H.P., Ayalon, A., Vonhof, H.B., Bar-Matthews, M., 2021. Eastern Mediterranean climate change deduced from the Soreq Cave fluid inclusion stable isotopes and carbonate clumped isotopes record of the last 160 ka. Quat. Sci. Rev. 272, 107223 https://doi.org/10.1016/j.quascirev.2021.107223.

Mischke, S., Opitz, S., Kalbe, J., Ginat, H., Al-Saqarat, B., 2015. Palaeoenvironmental inferences from late Quaternary sediments of the Al Jafr Basin. Jordan. Quat. Int. 382, 154–167. https://doi.org/10.1016/j.quaint.2014.12.041.

Mischke, S., Ginat, H., Al-Saqarat, B.S., Faershtein, G., Porat, N., Braun, P., Rech, J.A., 2017. Fossil-based reconstructions of ancient water bodies in the Levantine deserts. In: Bar-Yosef, O., Enzel, Y. (Eds.), Quaternary of the Levant: Environments, Climate Change, and Humans. Cambridge University Press, Cambridge, pp. 381–390. https://doi.org/10.1017/9781316106754.045.

Naor, H., Granit, Y., Zurieli, A., Burg, A., 2004. Southern Arava – updating of the hydrological and geochemical state of the aquifers and boreholes for the year 2003, operational forecast for 2007 and recommendations for new boreholes. Tahal Company Ltd Report 15046-d04.173, 62 p. (In Hebrew).

Petersen, J.O., Deschamps, P., Goncalves, J., Hamelin, B., Michelot, J.L., Guendouz, A., Zouari, K., 2014. Quantifying paleorecharge in the Continental Intercalaire (CI) aquifer by a Monte-Carlo inversion approach of 36Cl/Cl data. Appl. Geochem. 50, 209–221.

Priestley, S.C., Meredith, K.T., Treble, P.C., Cendón, D.I., Griffiths, A.D., Hollins, S.E., Baker, A., Pigois, J.-P., 2020. A 35 ka record of groundwater recharge in south-West Australia using stable water isotopes. Sci. Total Environ. 717, 135105 https://doi.org/10.1016/j.scitotenv.2019.135105.

Purtschert, R., Yokochi, R., Jiang, W., Lu, Z.T., Mueller, P., Zappala, J., Van Heerden, E., Cason, E., Lau, M., Kieft, T.L., Gerber, C., Brennwald, M.S., Onstott, T.C., 2021. Underground production of 81Kr detected in subsurface fluids. Geochim. Cosmochim. Acta 295, 65–79. https://doi.org/10.1016/J.GCA.2020.11.024.

Purtschert, R., Love, A.J., Jiang, W., Lu, Z.-T., Yang, G.-M., Fulton, S., Wohling, D., Shand, P., Aeschbach, W., Bröder, L., Müller, P., Tosaki, Y., 2023. Residence times of groundwater along a flow path in the Great Artesian Basin determined by 81Kr, 36Cl and 4He: implications for palaeo hydrogeology. Sci. Total Environ. 859, 159886 https://doi.org/10.1016/j.scitotenv.2022.159886.

Radulovic, M.M., Wong, H., Al Tarawneh, M., 2020. Groundwater flow modelling for an assessment of abstraction and climate change impacts on groundwater resources—an example from the Wadi Araba Basin (Jordan). Arab. J. Geosci. 13, 1142. https://doi.org/10.1007/s12517-020-06148-2.

Ram, R., Burg, A., Zappala, J.C., Yokochi, R., Yechieli, Y., Purtschert, R., Jiang, W., Lu, Z.-T., Mueller, P., Bernier, R., Adar, E.M., 2020. Identifying recharge processes into a vast "fossil" aquifer based on dynamic groundwater 81Kr age evolution. J. Hydrol. 587, 124946 https://doi.org/10.1016/j.jhydrol.2020.124946.

Ram, R., Purtschert, R., Adar, E.M., Bishof, M., Jiang, W., Lu, Z.-T., Mueller, P., Sy, A., Vockenhuber, C., Yechieli, Y., Yokochi, R., Zappala, J.C., Burg, A., 2021. Controls on the 36Cl/Cl input ratio of paleo-groundwater in arid environments: New evidence from 81Kr/Kr data. Sci. Total Environ. 762 https://doi.org/10.1016/j.scitotenv.2020.144106.

Ram, R., Solomon, D.K., Yokochi, R., Burg, A., Purtschert, R., Seltzer, A.M., Yechieli, Y., Zappala, J.C., Lu, Z.T., Jiang, W., Mueller, P., Adar, E.M., 2022. Large-scale paleo water-table rise in a deep desert aquifer recorded by dissolved noble gases. J. Hydrol. 612, 128114 https://doi.org/10.1016/j.jhydrol.2022.128114.

Ritterbusch, F., Ebser, S., Welte, J., Reichel, T., Kersting, A., Purtschert, R., Aeschbach-Hertig, W., Oberthaler, M.K., 2014. Groundwater dating with Atom Trap Trace Analysis of 39Ar. Geophys. Res. Lett. 41, 6758–6764. https://doi.org/10.1002/2014GL061120.

Rödiger, T., Geyer, S., Odeh, T., Siebert, C., 2023. Data scarce modelling the impact of present and future groundwater development on Jordan multiaquifer groundwater resources. Sci. Total Environ. 870, 161729 https://doi.org/10.1016/j.scitotenv.2023.161729.

Rosenthal, E., Adar, E., Issar, A.S., Batelaan, O., 1990. Definition of groundwater flow patterns by environmental tracers in the multiple aquifer system of southern Arava Valley. Israel. J. Hydrol. 117, 339–368.

Rosenthal, E., Zilberbrand, M., Livshitz, Y., 2007. The hydrochemical evolution of brackish groundwater in central and northern Sinai (Egypt) and in the western Negev (Israel). J. Hydrol. 337, 294–314. https://doi.org/10.1016/j.jhydrol.2007.01.042.

Rubin, S., Ziv, B., Paldor, N., 2007. Tropical plumes over eastern North Africa as a source of rain in the Middle East. Mon. Weather Rev. 135, 4135–4148. https://doi.org/10.1175/2007MWR1919.1.

Scanlon, B.R., Keese, K.E., Flint, A.L., Flint, L.E., Gaye, C.B., Edmunds, W.M., Simmers, I., 2006. Global synthesis of groundwater recharge in semiarid and arid regions. Hydrol. Process. 20, 3335–3370. https://doi.org/10.1002/hyp.6335.

Schulz, S., Walther, M., Michelsen, N., Rausch, R., Dirks, H., Al-Saud, M., Merz, R., Kolditz, O., Schüth, C., 2017. Improving large-scale groundwater models by considering fossil gradients. Adv. Water Resour. 103, 32–43. https://doi.org/10.1016/J.ADVWATRES.2017.02.010.

Seltzer, A.M., Ng, J., Danskin, W.R., Kulongoski, J.T., Gannon, R.S., Stute, M., Severinghaus, J.P., 2019. Deglacial water-table decline in Southern California recorded by noble gas isotopes. Nat. Commun. 10, 5739. https://doi.org/10.1038/s41467-019-13693-2.

Seltzer, A.M., Ng, J., Aeschbach, W., Kipfer, R., Kulongoski, J.T., Severinghaus, J.P., Stute, M., 2021. Widespread six degrees Celsius cooling on land during the Last Glacial Maximum. Nature 593, 228–232. https://doi.org/10.1038/s41586-021-03467-6.

Shentsis, I., Rosenthal, E., 2003. Recharge of aquifers by flood events in an arid region. Hydrol. Process. 17, 695–712. https://doi.org/10.1002/hyp.1160.

Sneh, A., Bartov, Y., Rosensaft, M., 1998. Geological Map of Israel 1:200,000 Geological Survey of Israel, Jerusalem.

Sonntag, C., Thorweihe, U., Rudolph, J., Löhnert, E.P., Junghans, C., Münnich, K.O., Klitzsch, E., El Shazly, E.M., Swailem, F.M., 1980. Paleoclimatic evidence in apparent 14C ages of Saharian groundwaters. Radiocarbon 22, 871–878. https://doi.org/10.1017/S0033822200010262.

Sturchio, N.C., Du, X., Purtschert, R., Lehmann, B.E., Sultan, M., Patterson, L.J., Lu, Z.-T., Müller, P., Bigler, T., Bailey, K., O'Connor, T.P., Young, L., Lorenzo, R., Becker, R., El Alfy, Z., El Kaliouby, B., Dawood, Y., Abdallah, A.M.A., 2004. One million year old groundwater in the Sahara revealed by krypton-81 and chlorine-36. Geophys. Res. Lett. 31, 2–5. https://doi.org/10.1029/2003GL019234.

Stute, M., Schlosser, P., 1993. Principles and applications of the noble gas paleothermometer. Clim. Chang. Cont. Isot. Rec. 78, 374.

Stute, M., Schlosser, P., 2000. Atmospheric noble gases. In: Cook, P.G., Herczeg, A.L. (Eds.), Environmental Tracers in Subsurface Hydrology. Springer, US, pp. 349–377.

Sultan, M., Sturchio, N., Hassan, F., Hamdan, M.R., Mahmood, M., El Alfy, Z., Stein, T., 1997. Precipitation source inferred from stable isotopic composition of Pleistocene

groundwater and carbonate deposits in the Western Desert of Egypt. Quat. Res. 48, 29–37. https://doi.org/10.1006/qres.1997.1907.
Sultan, M., Metwally, S., Milewski, A., Becker, D., Ahmed, M., Sauck, W., Soliman, F., Sturchio, N., Yan, E., Rashed, M., Wagdy, A., Becker, R., Welton, B., 2011. Modern recharge to fossil aquifers: Geochemical, geophysical, and modeling constraints. J. Hydrol. 403, 14–24. https://doi.org/10.1016/j.jhydrol.2011.03.036.
Tadros, C.V., Treble, P.C., Baker, A., Hankin, S., Roach, R., 2019. Cave drip water solutes in South-Eastern Australia: Constraining sources, sinks and processes. Sci. Total Environ. 651, 2175–2186. https://doi.org/10.1016/j.scitotenv.2018.10.035.
Tantawi, M.A., El-Sayed, E., Awad, M.A., 1998. Hydrochemical and stable isotope study of groundwater in the Saint Catherine-Wadi Feiran area, South Sinai. Egypt. J. African Earth Sci. 26, 277–284. https://doi.org/10.1016/S0899-5362(98)00010-4.
Vaks, A., Bar-Matthews, M., Ayalon, A., Matthews, A., Frumkin, A., Dayan, U., Halicz, L., Almogi-Labin, A., Schilman, B., 2006. Paleoclimate and location of the border between Mediterranean climate region and the Saharo-Arabian Desert as revealed by speleothems from the northern Negev Desert. Israel. Earth Planet. Sci. Lett. 249, 384–399. https://doi.org/10.1016/j.epsl.2006.07.009.
Vaks, A., Bar-Matthews, M., Ayalon, A., Matthews, A., Halicz, L., Frumkin, A., 2007. Desert speleothems reveal climatic window for African exodus of early modern humans. Geology 35, 831–834. https://doi.org/10.1130/G23794A.1.
Vaks, A., Bar-Matthews, M., Matthews, A., Ayalon, A., Frumkin, A., 2010. Middle-late Quaternary paleoclimate of northern margins of the Saharan-Arabian Desert: Reconstruction from speleothems of Negev Desert. Israel. Quat. Sci. Rev. 29, 2647–2662. https://doi.org/10.1016/j.quascirev.2010.06.014.
Vaks, A., Bar-Matthews, M., Ayalon, A., Matthews, A., Frumkin, A., 2018. Pliocene–Pleistocene palaeoclimate reconstruction from Ashalim Cave speleothems, Negev Desert, Israel. Geol. Soc. London, Spec. Publ. 466, 201 LP – 216. doi:https://doi.org/10.1144/SP466.10.
van Rooyen, J.D., Watson, A.W., Miller, J.A., 2022. Using tritium and radiocarbon activities to constrain regional modern and fossil groundwater mixing in southern Africa. J. Hydrol. 614, 128570 https://doi.org/10.1016/j.jhydrol.2022.128570.
Vengosh, A., Hening, S., Ganor, J., Mayer, B., Weyhenmeyer, C.E., Bullen, T.D., Paytan, A., 2007. New isotopic evidence for the origin of groundwater from the Nubian sandstone aquifer in the Negev. Israel. Appl. Geochem. 22, 1052–1073.
Vengosh, A., Rimawi, O., Al-Zoubi, A., Marie, A., Ganor, J., 2010. A multi-isotope (radium, boron, strontium, sulfur, carbon, oxygen, hydrogen) investigation of fossil groundwater from the Disi Aquifer in southern Jordan: Tracing water sources, water-rock interactions, and residence time. AGU Fall Meeting Abstracts 2010, H21L–03.
Waldmann, N., Torfstein, A., Stein, M., 2010. Northward intrusions of low- and mid-latitude storms across the Saharo-Arabian belt during past interglacials. Geology 38, 567–570. https://doi.org/10.1130/G30654.1.
Weyhenmeyer, C.E., Burns, S.J., Waber, H.N., Aeschbach-Hertig, W., Kipfer, R., Loosli, H. H., Matter, A., 2000. Cool glacial temperatures and changes in moisture source recorded in Oman groundwaters. Science 287, 842–845. https://doi.org/10.1126/science.287.5454.842.
Yehudai, M., Lazar, B., Bar, N., Kiro, Y., Agnon, A., Shaked, Y., Stein, M., 2017. U–Th dating of calcite corals from the Gulf of Aqaba. Geochim. Cosmochim. Acta 198, 285–298. https://doi.org/10.1016/j.gca.2016.11.005.
Yokochi, R., 2016. Recent developments on field gas extraction and sample preparation methods for radiokrypton dating of groundwater. J. Hydrol. 540, 368–378.
Yokochi, R., Bernier, R., Purtschert, R., Zappala, J.C., Yechieli, Y., Adar, E., Jiang, W., Lu, Z.-T., Mueller, P., Olack, G., Ram, R., 2018. Field degassing as a new sampling method for 14C analyses in old groundwater. Radiocarbon 60, 349–366. https://doi.org/10.1017/RDC.2017.64.
Yokochi, R., Ram, R., Zappala, J.C., Jiang, W., Adar, E., Bernier, R., Burg, A., Dayan, U., Lu, Z.-T., Mueller, P., Purtschert, R., Yechieli, Y., 2019. Radiokrypton unveils dual moisture sources of a deep desert aquifer. Proc. Natl. Acad. Sci. 116, 16222–16228. https://doi.org/10.1073/pnas.1904260116.
Yousif, M., Hussien, H.M., Abotalib, A.Z., 2020. The respective roles of modern and paleo recharge to alluvium aquifers in continental rift basins: A case study from El Qaa plain, Sinai. Egypt. Sci. Total Environ. 739, 139927 https://doi.org/10.1016/j.scitotenv.2020.139927.
Zappala, J.C., McLain, D., Mueller, P., Steeb, J.L., 2020. Enhanced detection limits for radiokrypton analysis. J. Radioanal. Nucl. Chem. https://doi.org/10.1007/s10967-020-07355-7.